



Contents lists available at ScienceDirect

Journal of Advanced Research

journal homepage: www.elsevier.com/locate/jare

Dual function of MrgprB2 receptor-dependent neural immune axis in chronic pain

Yucui Jiang^{a,1}, Fan Ye^{d,1}, Jian Zhang^{b,1}, Yun Huang^b, Yingxin Zong^b, Feiyan Chen^a, Yan Yang^b, Chan Zhu^b, Tao Yang^c, Guang Yu^{b,*}, Zongxiang Tang^{b,*}

^aSchool of Chinese Medicine, Nanjing University of Chinese Medicine, 138 Xianlin Road, Nanjing 210023, China

^bSchool of Medicine, Nanjing University of Chinese Medicine, 138 Xianlin Road, Nanjing 210023, China

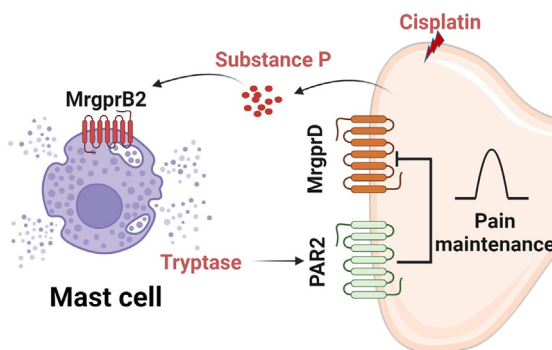
^cState Key Laboratory of Organic Electronics and Information Displays & Institute of Advanced Materials (IAM), Nanjing University of Posts & Telecommunications, 9 Wenyuan Road, Nanjing 210023, China

^dCollege of Pharmacy, Jishou University, Jishou 416000, China

HIGHLIGHTS

- Substance P/MrgprB2/Tryptase/PAR2 pathway contributes to the formation of cisplatin-induced neuropathic pain.
- PAR2 and MrgprD are partially co-expressed in DRG neurons with mutual restraint.
- Knocking out MrgprD could alleviate cisplatin-induced neuropathic pain.
- MrgprB2 activation contributed to the pain recovery at the later stage of CINP by down-regulating MrgprD receptor.

GRAPHICAL ABSTRACT



ARTICLE INFO

Article history:

Received 26 March 2024

Revised 26 November 2024

Accepted 26 February 2025

Available online xxx

Keywords:

CINP
MrgprB2 receptor
PAR2 receptor
MrgprD receptor

ABSTRACT

Introduction: Neuro-immune interactions have been recognized to be involved in the development of neuropathic pain induced by chemotherapeutic drugs (CINP). However, its role in pain resolution remains largely unknown, particularly concerning mast cells.

Objectives: To investigate the bidirectional modulation of mast cell Mas-related G protein-coupled receptor B2 (MrgprB2)-mediated neuro-immune interactions in CINP.

Methods: CINP model was established in wild-type mice, Mas-related G protein-coupled receptor D knockout (MrgprD^{-/-}) mice, mast cell-deficient mice, MrgprB2 knockout (MrgprB2^{-/-}) mice, and MrgprB2-Cre tdTomato mice. The role of MrgprB2 receptor in CINP was investigated by calcium imaging, cytokine antibody arrays, mining of single-cell sequencing databases, immunofluorescence, western blotting, co-immunoprecipitation (Co-IP), among other methodologies.

Results: We observed that cisplatin-induced allodynia was significantly inhibited in MrgprB2^{-/-} mice, which was attributed to the blockade of tryptase release and the suppression of upregulation of protease-activated receptor 2 (PAR2) expression in dorsal root ganglion (DRG). Thus, the activation of MrgprB2/Tryptase/PAR2 axis contributed to the development of cisplatin-induced pain. In addition, we

Abbreviations: CINP, Chemotherapy-induced neuropathic pain; MrgprB2, mas-related G protein-coupled receptor B2; MrgprD, mas-related G protein-coupled receptor D; Co-IP, Co-Immunoprecipitation; SP, Substance P; PAR2, proteinase activated receptor-2; GPCR, G protein-coupled receptor; IB4, plant lectin B4; CCI, chronic constriction; MrgprX2, mas-related G protein-coupled receptor X2; AD, Atopic Dermatitis; ACD, Atopic Contact Dermatitis; DRG, Dorsal root ganglion; CIPN, Chemotherapy-induced peripheral neuropathy; CFA, complete Freund's adjuvant; TRP, transient receptor potential; PAMP, Proadrenomedullin N-terminal 20 peptide.

* Corresponding authors.

E-mail addresses: yuguang@njucm.edu.cn (G. Yu), njucm_m_t@njucm.edu.cn (Z. Tang).

¹ These authors contributed equally this paper.

<https://doi.org/10.1016/j.jare.2025.02.037>

2090-1232/© 2025 Published by Elsevier B.V. on behalf of Cairo University.

This is an open access article under the CC BY-NC-ND license (<http://creativecommons.org/licenses/by-nc-nd/4.0/>).

also found that there was co-expression of PAR2 and MrgprD in DRG neurons. And activation of PAR2 can negatively regulate the expression of MrgprD, whether in a physiological state or in a chronic pain condition. Consequently, MrgprD expression was down-regulated by the activation of the MrgprB2/Tryptase/PAR2 axis during the later stages of CINP, which was associated with pain relief. Therefore, the activation of MrgprB2/Tryptase/PAR2 axis also contributed to the alleviation of cisplatin-induced pain. This finding was in line with the phenomenon that persistent stimulation by cisplatin did not cause a continuous increase in pain.

Conclusions: Our research elucidated the bidirectional modulation of MrgprB2-dependent neural immune axis in CINP. This study emphasized that MrgprB2 is a critical target for early intervention in CINP, and highlighted the necessity of considering the mechanism differences at different stages in pain management.

© 2025 Published by Elsevier B.V. on behalf of Cairo University. This is an open access article under the CC BY-NC-ND license (<http://creativecommons.org/licenses/by-nc-nd/4.0/>).

Introduction

Neuropathic pain (NP) is an important public health problem that negatively impacts quality of life and exacts an enormous socio-economic cost [1]. Chemotherapy-induced peripheral neuropathy (CIPN) is a common dose-limiting adverse side effect and results in high incidence of neuropathic pain [2]. The prevalence of chemotherapy-induced peripheral neuropathy (CIPN) varies among individuals, with reported rates ranging from 19 % to over 85 %. The highest prevalence is observed in patients receiving platinum-based medications (70–100 %), followed by those treated with taxanes (11–87 %), ixabepilone (60–65 %), and thalidomide along with its analogs (20–60 %) [3]. CIPN has a direct impact on the survival and quality of life due to its long-lasting nature [4]. Prevention or treatment of CIPN is still an unmet clinical need due to the incomplete understanding of the pathogenesis of CIPN [5,6]. It is well established that neuro-immune interaction is a potential common driver of neuropathic pain caused by chemotherapy drugs [7]. Activation of mast cells has been shown to play an important role in neuropathic pain induced by vincristine [8], oxaliplatin [9], and paclitaxel [10]. Emerging evidence indicates that specific subtypes of immune cells, such as antinociceptive macrophages and T regulatory cells, can contribute to pain resolution [11]. Hence, in addition to the development of CINP, whether mast cells are also involved in the resolution of CINP remains to be investigated.

MrgprB2 is selectively expressed on connective tissue mast cells. It can be activated by various basic secretagogues through a non-IgE mechanism, including inflammatory peptides and drugs associated with allergic reactions [12]. MrgprB2 and MrgprX2 play important roles in skin host defense, but their inappropriate activation contributes to the pathogenesis of rosacea, AD, ACD, non-histamine pruritus, pseudo hypersensitivity, and mastocytosis [13]. MrgprB2/MrgprX2 is also associated with the development of pain. MrgprB2 receptor has been shown to play an important role in the postoperative pain by mediating the release of chemokines CCL2/CCL3 from mast cells [14]. MrgprB2 receptor can also sensitize TRPV1 channels in neurons through mediating TNF- α release, thereby contributing to alcohol-withdrawal-associated headaches [15]. Furthermore, Pituitary Adenylate Cyclase Activating Peptide (PACAP) can also mediate mast cell activation via the activation of MrgprB2 receptor, thus contributing to migraine development [16]. Therefore, we speculate that the activation of MrgprB2 may also play important roles in CINP. In addition, it has been reported that MrgprB2 is capable of mediating the release of tryptase [17]. Tryptase, the most abundant protease of the mast cell, has been implicated as a key mediator of pain that acts through activation of its cognate receptor PAR2. The tryptase-

PAR2 axis plays important roles in nociceptive signaling and pain [18]. Numerous studies have shown that PAR2 is involved in neuropathic pain induced by a variety of chemotherapy drugs, such as bortezomib [19], oxaliplatin [20], paclitaxel [10]. Consequently, we hypothesize that the MrgprB2/Tryptase/PAR2 axis might be implicated in the progression of CINP.

Studies have shown that PAR2 and Mrgprs are partially co-expressed in DRG neurons, and that activation of PAR2 can regulate the function of Mrgprs [21]. In addition, the activation of MrgprB2 can predominantly stimulate DRG neurons that overlap with MrgprD⁺ neurons [17], indicating MrgprB2/Tryptase/PAR2 axis may regulate MrgprD receptor in DRG neurons. MrgprD is expressed within IB4⁺ DRG neurons and has been proposed to be involved in pain sensation and modulation [22]. Genetic ablation in adulthood of unmyelinated sensory neurons expressing the MrgprD reduces behavioral sensitivity to noxious mechanical stimuli but not to heat or cold stimuli [23]. MrgprD also participates in inflammatory pain by facilitating NF- κ B activation through interaction with TAK1 and IKK complex [24]. Also, our previous study has found that MrgprD plays an important role in the cold pain of CCI-induced neuropathic pain through the PKA-TRPA1 pathway [25]. Additionally, reports demonstrate that there is a downregulation of MrgprD expression in some chronic diseases, such as SNL-induced neuropathic pain [26]. This implies that the body itself could alleviate pain by downregulating the expression of MrgprD. Furthermore, we observed that regardless of whether in the later stages of postoperative pain [14] or migraine [16], wild-type mice exhibited a rapid recovery in pain behavior. In contrast, MrgprB2^{-/-} mice demonstrated a slower recovery in pain behavior. This suggests that the presence of MrgprB2 may be beneficial to the process of pain recovery. Hence, we hypothesize that the MrgprB2 receptor might also contribute to pain alleviation by negatively regulating MrgprD receptor through PAR2 receptor.

In the current study, we explored the role of neuron-mast cell interactions in the formation and resolution of CINP. Our findings demonstrated that the MrgprB2/Tryptase/PAR2 axis not only contributed to cisplatin-induced pain hypersensitivity, but also alleviated pain during the later stages of CINP by down-regulating the expression of MrgprD.

Material and methods

Ethics statement

All animal procedures were approved by the Institutional Animal Care & Use Committee (IACUC) of Nanjing University of Chinese Medicine (Permit No. ACU210406).

Animals

Adult C57BL/6J male mice (8–10 weeks) were purchased from Charles River; Mast cell-deficient Kit (W-sh)/Kit (W-sh) sash mice, MrgprB2^{-/-} mice, MrgprD^{-/-} mice, MrgprB2-Cre tdT mice, MrgprD-Cre tdT mice were kindly provided by Xinzhong Dong (Johns Hopkins University, Baltimore). Most experiments were performed on male mice between the ages of 8–12 weeks. Additionally, comparative experiments on pain behavior in C57BL/6J mice and MrgprB2^{-/-} mice were conducted among both female and male mice.

Chronic pain model

Cisplatin-induced pain model: Mice with different genotypes (WT mice, MrgprD^{-/-} mice, mast cell-deficient mice, MrgprB2^{-/-} mice) were randomly divided into normal saline group and cisplatin group, and no less than 5 mice in each group were used for behavioral assessment. Additionally, in the inhibitor intervention experiments, CINP mice were randomly divided into solvent group and drug group, with no less than 4 mice in each group for behavioral assessment. Model mice were administered with cisplatin (0.8 mg/kg, intraperitoneal injection, i.p., once daily, from day 0 to day 11 for a total of 12 consecutive days) to induce chemotherapy-related neuropathic pain [27]. Mice in normal saline group were administered with normal saline via intraperitoneal injection. Behavioral assessments were conducted 24 h after cisplatin treatment. The samples were collected at the different stages of pain progression: the initial phase of pain (day 3), the development phase of pain (day 7), and the dynamic equilibrium phase of pain (day 11).

Postoperative pain model: WT mice were randomly divided into sham group and model group, with 5 mice in each group. The postoperative pain model was established according to the literature of Green et al. [14]. Initially, the right hind leg of mice was disinfected with iodophor solution after anesthesia. Subsequently, an 11- scalpel blade was employed for a longitudinal incision. The incision commenced about 2 mm from the proximal end of the heel and extended towards the toes. The incision length was about 5 mm. Meanwhile, the underlying muscle was carefully elevated using curved forceps, ensuring that both the origin and insertion of the muscle remained intact. Finally, 8–0 nylon mattress suture was used to complete the skin closure, and then an erythromycin ointment was applied to the wound. Mice in the sham group were anesthetized, disinfected and treated with erythromycin ointment without any incision. Behavioral assessments were conducted 24 h after the incision, and samples were collected during the period of pain recovery (day 5).

Complete Freund's Adjuvant (CFA) pain model: WT mice were randomly divided into sham group and model group, with 5 mice in each group. Mice in the model group were injected with 10 μ L Complete Freund's Adjuvant (Sigma, USA, F5881) to the right hind paw (subcutaneous injection, i.h.). Mice in normal saline group were administered with 10 μ L normal saline (i.h.). Behavioral assessments were conducted 24 h after the incision, and samples were collected during the period of pain recovery (day 5).

Behavioral assays

In the CINP pain model, the mechanical allodynia, thermal hyperalgesia, and cold allodynia of each group of mice were evaluated. In the reference literature [14], the mechanical allodynia of each group of mice were evaluated in the postoperative pain model and CFA pain model. Each behavior assessment was performed every other day.

Measurement of mechanical allodynia: As our previous study described [28], the withdrawal threshold was defined as the frequency of paw withdrawal responses to a standard von Frey hairs that delivered a force of 0.16 g (Ugo Basile, Gemonio, Italy).

Measurement of heat hyperalgesia: Heat hyperalgesia was evaluated by radiant heat (Ugo Basile, Gemonio, Italy). Animals were habituated to the testing environment for at least 2 days before testing. Mice were placed in elevated glass platform and allowed to habituate for 30 min. The radiant heat source was applied to the hind paw with intervals of at least 3 min between applications. A cutoff time of 20.1 s was imposed to prevent tissue damage. The average withdrawal latency was recorded as the response latency.

Measurement of cold allodynia: Cold allodynia was evaluated by cold plate testing [29]. Animals were habituated to the testing environment for at least 2 days before testing. Each animal was placed on a cold plate maintained at $4 \pm 1^\circ\text{C}$, brisk lifting of the hindpaw was counted as a nociceptive response, and the number of lifts within 5 min was counted. Walking steps or slow paw lifting related to locomotion were not counted.

Histological assays

In the CINP model, we collected paw tissues for histological assays at day 0, day 3, day 7 and day 11. Histological assays, including Hematoxylin-Eosin staining and Toluidine blue staining, were performed as described in our previous study [28].

Quantitative real-time PCR

In the CINP model, the paw tissues and DRGs for qPCR were collected at day 0, day 3, day 7 and day 11. Total RNA was extracted by using the TRIzol (Vazyme, Nanjing, China, R401-01) method. Complementary DNA (cDNA) was generated by using Hifair[®] II One Step RT-qPCR SYBR Green Kit (Yeasen, Shanghai, China) according to the manufacturer's instruction. Real-time qPCR was performed by using Hieff[®] qPCR SYBR Green Master Mix (Yeasen, Shanghai, China) and GAPDH were used as the internal controls. The sequences of the mouse MrgprB2 primers were as follows: forward, 5'-AATCAAGAATCTAAGCACCTC-3', and reverse, 5'-CGTTTACAGCGATACCAA-3'. The sequences of the mouse PAR2 primers were as follows: forward, 5'-CGGGACGCAACAACAGTAAAGGA-3', and reverse, 5'-AGGGGAACCAGATGACAGAGAG-3'. The sequences of the mouse MrgprD primers were as follows: forward, 5'-TGTGGGGGGATGGCAGGCAAC-3', and reverse, 5'-ATGGGGAAAAGCACGGAGAGGC-3'. The sequences of the mouse GAPDH primers were as follows: 5'-GCACAGTCAAGGCCGAGAAT-3', and reverse, 5'-GCCTTCTCCATGGTGGTGAA-3'.

Western blot

In the CINP model, the paw tissues and DRGs for western blot were collected at day 0, day 3, day 7 and day 11. Tissues were homogenized in Radio-Immunoprecipitation Assay (RIPA) lysis buffer containing a mixture of protease inhibitors and Phenylmethyl sulfonyl fluoride (PMSF) (Beyotime, Shanghai, China, P0013B). The homogenate was then ultrasonic and centrifuged. The protein samples were separated on 10 % SDS-PAGE gels (Beyotime, Shanghai, China, P0012A) and transferred to the polyvinylidene fluoride (PVDF) membranes (Millipore, USA, IPFL00010). Then the membranes were blocked by 5 % Bovine Serum Albumin (BSA) (Solarbio, Beijing, China, A8010), and probed with primary antibodies, followed by Horseradish Peroxidase (HRP)-conjugated secondary antibodies. GAPDH, β -Actin or β -Tubulin as a loading control. Signals were visualized using Super ECL Detection Reagent (Yeasen, Shanghai, China, 36208ES60), and captured by ChemiDoc XRS system (Bio-Rad, USA). Primary antibodies we used as follow-

ing: mouse anti-PAR2 (1:1000, Santa Cruz, sc-13504), mouse anti-tryptase (1:1000, Santa Cruz, sc-59587), rabbit anti-MrgprD (1:1000, Alomone, AMR-061), rabbit anti-GAPDH (1:5000, Absin, abs-124037), mouse anti- β -Actin (1:5000, FUDE, FD0060-50), mouse anti- β -Tubulin (1:5000, FUDE, FD0064-50). Image J was used to measure the gray value of the specific bands.

Immunofluorescence

In the CINP model, the paw tissues and DRGs for immunofluorescence were collected at day 0, day 3, day 7 and day 11. Tissues were fixed in 4 % paraformaldehyde for 24 h at 4°C and then dehydrated in sucrose for 24 h at 4°C. The sections were embedded in OCT and sliced to a thickness of 10 μ m. The sections were fixed with 4 % paraformaldehyde at RT for 10 min. The slides were processed by 0.15 % Triton X-100 for 20 min at RT (for substance P and tryptase staining), and then blocked with 3 % BSA for 1 h at 37°C. Then the slides incubated for overnight at 4°C with mouse anti-substance P (1:500, R&D), mouse anti-tryptase (1:500, Santa Cruz, sc-59587), mouse anti-PAR2 (1:500, Santa Cruz, sc-13504), rabbit anti-MrgprD (1:500, Alomone, AMR-061), mouse monoclonal anti-substance P (1:500, R&D, MAB4375) or a mixture of mouse anti-PAR2 (1:500, Santa Cruz) and rabbit anti-MrgprD (1:500, Alomone). The sections were then incubated with Alexa Fluor 555/488-conjugated anti-mouse IgG (H + L) antibody, or Alexa Fluor 555-conjugated anti-rabbit IgG (H + L) antibody, or a mixture of Alexa Fluor 555-conjugated anti-mouse IgG (H + L) antibody and Alexa Fluor 488-conjugated anti-rabbit IgG (H + L) antibody (1:200, Beyotime) for 2 h at 37°C. For hindpaw tissues sections, FITC-avidin staining was followed for 30 min after tryptase staining. Then the sections were mounted with Antifade Mounting Medium with DAPI (Beyotime, Shanghai, China, P0131) and images captured with the microscope (Nikon, Tokyo, Japan) with a magnification of 125 or 200.

Substance p ELISA

Substance P ELISA (Mlbio) was prepared according to the manufacturer's protocol. Briefly, whole DRG tissues were harvested at the development phase of pain (day 7) after cisplatin treatment. Then the tissues were homogenized in PBS. After homogenization, the supernatant was collected and stored at 80°C until used for ELISA.

Cytokine antibody array

The cytokine antibody array is capable of simultaneously detecting 111 types of mouse cytokines in a single experiment. This array exhibits sensitivity at the pg/mL level. Similar to ELISA, the antibody array is also based on the measurement of antibody pairs. Compared to conducting multiple ELISA or western blot experiments, the time and cost associated with using an antibody array are significantly lower. Therefore, we employed cytokine antibody array technology to assess the expression of various inflammatory factors in different groups of mice. Referring to the literature [30], hindpaw tissues at the development phase of pain (day 7) were homogenized in PBS containing protease inhibitors. After homogenization, Triton X-100 was added to the homogenates (final concentration of 1 %), frozen at -80 °C for 1 day, then thawed and centrifuged at 12000 rpm for 30 min at 4 °C to remove cellular debris. After protein quantitation with BCA protein assay kit, hindpaw tissues homogenates were harvested and mixed at equal quantity, and 200 μ g total protein were used. The mixed homogenates were assayed by the Proteome Profiler Mouse XL Cytokine Array (R&D Systems, USA, ARY028) according to the manufacturer's recommendation.

Culture of mouse DRG neurons

The mice were deeply anesthetized with overdoses of isoflurane. Mouse DRGs were collected in cold DH10 medium (DMEM/F-12 with 10 % fetal bovine serum and 1 % penicillin-streptomycin) and digested with collagenase type I (1.6 mg/mL, Sigma) and dispase-II (3.5 mg/mL, Sigma) for 30 min at 37°C. After blowing, filtration and centrifugation, DRGs were suspended in DH10 medium. Then the cells were plated on glass cover slips coated with poly-D-lysine (0.5 mg/mL, solarbio, P2100) and laminin (10 μ g/mL, Sigma, 11243217001). DRG Neurons were cultured in fresh DH10 medium with nerve growth factor (50 ng/mL, Sigma) at 37°C and used within 24 h.

Calcium imaging

DRG neurons were incubated with 2 μ M Fura-2 AM (Sigma, 47989) and 0.02 % Pluronic F-127 (Sigma, P2443) at 37°C for 17 min or 2 μ M Fluo-4 AM (Beyotime, S1060) and 0.02 % Pluronic F-127 (Sigma, P2443) at RT for 30 min. The cells then immediately washed 3 times by calcium imaging buffer (137 mM NaCl, 5.4 mM KCl, 1 mM CaCl₂, 1.2 mM MgCl₂, 8 mM glucose, 1.2 mM NaH₂PO₄, 20 mM HEPES, PH was 7.4). A high-speed, continuously scanning, monochromatic light source (Polychrome V, Till Photonics, Grafelfing, Germany) was used for excitations of 340/380 nm or 488 nm (2 s exposure time), enabling the detection of changes in the intracellular free calcium concentration. Each experiment was done at least 4 times and at least 100 cells were analyzed each time. The intensity of the cell response to the agonists was quantified by the fluorescence intensity ratio. The fluorescence intensity ratio = (F_{max} - F₀) / (F₀), where F_{max} represented the maximum value of fluorescence, and F₀ was the baseline fluorescence. The proportion of the cell response to the agonists was quantified by the ratio of positive cells to the total number of cells.

Co-immunoprecipitation assays

The DRG lysate was incubated at 4°C for 2 h with 1.0 μ g anti-PAR2 or anti-IgG antibody, and then 20 μ L protein A/G PLUS-agarose beads (Santa Cruz Biotechnology) were added and incubated at 4°C for 4 h. Then beads were washed four times with immunoprecipitation buffer and analyzed by Western Blot.

Mining and analysis of single cell sequencing database

Cellular heterogeneity is a common characteristic of biological tissues, particularly in neurons. Traditional transcriptomic sequencing (RNA-Seq) and QPCR are limited to detecting transcriptional differences between individuals or populations, while the transcriptional variations at the cellular level remain challenging to assess accurately. Single-cell transcriptomics offers a novel approach for high-throughput sequencing at the individual cell level, effectively addressing the issue of transcriptional differences among cells. Therefore, we conducted an analysis of single-cell sequencing databases to investigate the expression levels of PAR2 and MrgprD receptors in each DRG neuron. The read counts for each coding gene for single-cell RNA-sequencing profiles of mouse DRG sensory neurons were obtained from Gene Expression Omnibus (accession number GSE63576). Clustering and visualization of the single-cell data sets were performed using Principal Components Analysis.

Statistical analysis

All data were presented as mean \pm SEM and analyzed using Prism 8.0 (GraphPad Software) and n represents the number of

mice analyzed. Statistical comparisons were conducted by two tails, unpaired Student's *t*-test (two groups) or one-way ANOVA analysis (more than two groups), and $p < 0.05$ was considered to be significant difference.

Results

MrgprB2 receptor is involved in cisplatin-induced neuropathic pain

Mast cells play crucial roles in the CINP induced by vincristine, oxaliplatin, and paclitaxel [8–10]. *MrgprB2* receptor is a key receptor specifically expressed on mast cells and is associated with the progression of inflammatory pain and headache. Therefore, in this study, we investigated the role of *MrgprB2* in CINP. As Fig. 1A–C illustrated, the mice showed obvious cold, mechanical allodynia, as well as thermal hypersensitivity after cisplatin stimulation. In addition, the infiltration of inflammatory cells and mast cells in the hindpaw tissues of model mice was significantly increased (Fig. S1A–B), and deleting mast cells could significantly reduce the pain induced by cisplatin (Fig. S1C–E). Compared to C57BL/6J mice, the cold allodynia in mast cell-deficient mice was significantly alleviated (Fig. S1C). However, there was no notable relief observed for mechanical allodynia, heat hyperalgesia, or weight loss (Fig. S1D–E, Fig. S2A). These findings underscore the importance of mast cells in cisplatin-induced cold pain.

Next, the function of *MrgprB2* was studied. We found that the infiltration of *MrgprB2*⁺ mast cells in the hindpaw tissues and DRGs was significantly increased (Fig. 1E). And real-time PCR results showed that the mRNA expression of *MrgprB2* receptor in hindpaw tissues of the model mice was also significantly up-regulated (Fig. 1D). Compared to C57BL/6J mice, *MrgprB2*^{−/−} female or male mice could significantly alleviate cisplatin-induced cold allodynia (Fig. 1F and 1I). At the same time, cisplatin-induced mechanical allodynia (Fig. 1G and 1J) and thermal hypersensitivity (Fig. 1H and 1K) in *MrgprB2*^{−/−} mice was also reduced to a certain extent. However, similar to sash mice, *MrgprB2*^{−/−} female or male mice could not significantly improve the weight loss induced by cisplatin (Fig. S2B–C). Moreover, compared to C57BL/6J mice, we also observed that *MrgprB2*^{−/−} mice had reductions in the infiltration of inflammatory cells induced by cisplatin (Fig. S3A, B). This may be due to reduced chemokines expression in *MrgprB2*^{−/−} model mice, such as CCL3/4, CXCL1, CXCL9, CXCL10, CXCL11, CXCL13 (Fig. 1M, Fig. S3C–H). Substance P could promote innate immune cell recruitment via activation of *MrgprB2* receptor in postoperative incision model [14], so we suggested that substance P might also be involved in the cisplatin-induced pain model. Immunofluorescence and ELISA results showed that cisplatin could increase the expression of substance P (Fig. 1L–O). Anti-substance P antibodies treatment (2 μg Anti-SP/20 μL saline, i.h., pretreatment for 1 h) could alleviate *MrgprB2*⁺ mast cells degranulation (Fig. S4A) and reduce pain hypersensitivity in model mice (Fig. 1P–R). Knocking out *MrgprB2* could reduce the analgesic effect of substance P antibody (Fig. S4B–D). Therefore, we suggested that *MrgprB2* might be activated by substance P to recruit inflammatory cells and participate in cisplatin-induced pain.

MrgprB2/Tryptase/PAR2 axis participates in cisplatin-induced neuropathic pain

Tryptase, the most abundant protease of mast cells, regulates neuronal activity by activating PAR2 receptor through protease cleavage. Having established that mast cell tryptase-PAR2 axis had important roles in nociceptive signaling and pain [18,31]. Previously, studies have shown that mast cell *MrgprB2* activation can

promote tryptase release [17]. We speculated that *MrgprB2*/Tryptase/PAR2 axis was involved in cisplatin-induced pain. Results showed that the expression of tryptase and β-tryptase in hindpaw tissues at different time points were significant increases in model group (Fig. 2A–C). Meanwhile, similar results were observed in DRGs of model mice (Fig. 2D–F). We also saw a significant increase of tryptase-positive cells co-stained with mast cell marker avidin in the hindpaw tissues of model mice (Fig. 2G). Additionally, blocking tryptase with APC366 could significantly reduce the cold allodynia and thermal hypersensitivity induced by cisplatin, and also inhibit the mechanical allodynia to a certain extent, indicating the important roles of tryptase in cisplatin-induced neuropathic pain (Fig. 2N–P). However, the tryptase expression in hindpaw tissues (Fig. 2H–J) or DRGs (Fig. 2K–M) was not increased in *MrgprB2*^{−/−} mice after modeling. Furthermore, immunofluorescence results of hindpaw tissues also showed that there was no significant increase of tryptase-positive cells co-stained with avidin in *MrgprB2*^{−/−} model mice (Fig. 2Q).

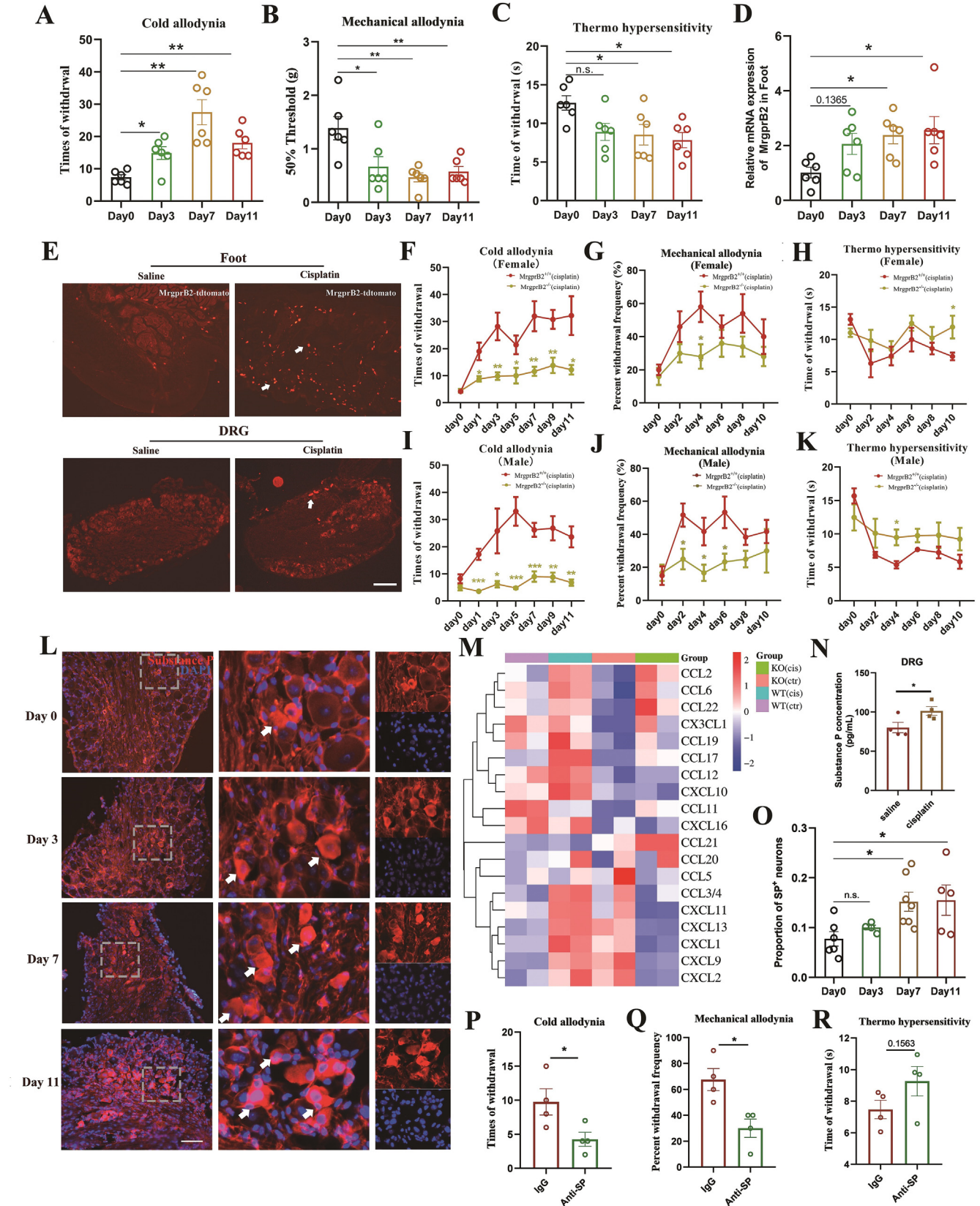
Then the role of PAR2 receptor in cisplatin-induced pain was examined. As we expect, PAR2 expression was significantly increased in model mice (Fig. 3A–D). In addition, blocking PAR2 receptor with FSLRRY-NH₂ significantly alleviated cisplatin-induced pain (Fig. 3E–G). Moreover, there were no change of PAR2 expression in *MrgprB2*^{−/−} mice after modeling (Fig. 3H–J). These results indicated that *MrgprB2* was involved in cisplatin-induced pain via Tryptase/PAR2 axis.

PAR2 receptor and *MrgprD* receptor are partially co-expressed in DRG neurons

The above results suggested that the *MrgprB2*/Tryptase/PAR2 axis was involved in the development of CINP. Studies have shown that PAR2 is partially co-expressed with *Mrgpr*s receptors in DRG neurons, and that PAR2 activation can regulate the function of *Mrgpr*s receptors [21]. In addition, the activation of *MrgprB2* mainly stimulates DRG neurons that overlap with *MrgprD*⁺ neurons which are implicated in pain sensation and modulation [22]. Based on these findings, we hypothesized that PAR2 may be involved in cisplatin-induced pain by regulating *MrgprD*. Then the co-expression of the receptors PAR2 and *MrgprD* was explored. We performed an analysis in WT mice, *MrgprB2*^{−/−} mice, *MrgprD*-Cre tdT mice, and *MrgprD*^{−/−}-eGFP mice to evaluate their co-expression pattern in DRG neurons. Immunofluorescence results showed that about 30–50 % of PAR2-positive neurons in different genotypes of mice expressed *MrgprD* (or eGFP) (Fig. 4A–G), which was similar to single-cell sequencing data (GSE63576, 27.2 % PAR2-positive neurons expressed *MrgprD* in C57/BL6J mice) (Fig. 4J–L). In addition, we also observed a population of DRG neurons isolated from WT mice (about 5 % of total DRG neurons) could respond to both β-alanine and SLIGRL-NH₂ stimulation, which further indicating PAR2 and *MrgprD* were partially co-expressed (Fig. 4H, I).

PAR2 receptor and *MrgprD* receptor are mutually restricted in DRG neurons

The above results showed that PAR2 and *MrgprD* receptors were partially co-expressed. Hence, we further investigated the potential regulatory role of PAR2 on *MrgprD* in the subsequent studies. Interestingly, we discovered that the regulation of PAR2 on *MrgprD* was negative. Compared with untreated WT mice, we found an increase in PAR2 mRNA expression and a decrease in *MrgprD* mRNA expression in whole DRGs of untreated *MrgprB2*^{−/−} mice (Fig. 5A–C). Pearson correlation analysis showed that the mRNA expression of PAR2 and *MrgprD* was negatively correlated (Fig. 5D). Similarly, we also observed that PAR2 expression was up-regulated and *MrgprD* expression was down-regulated at the



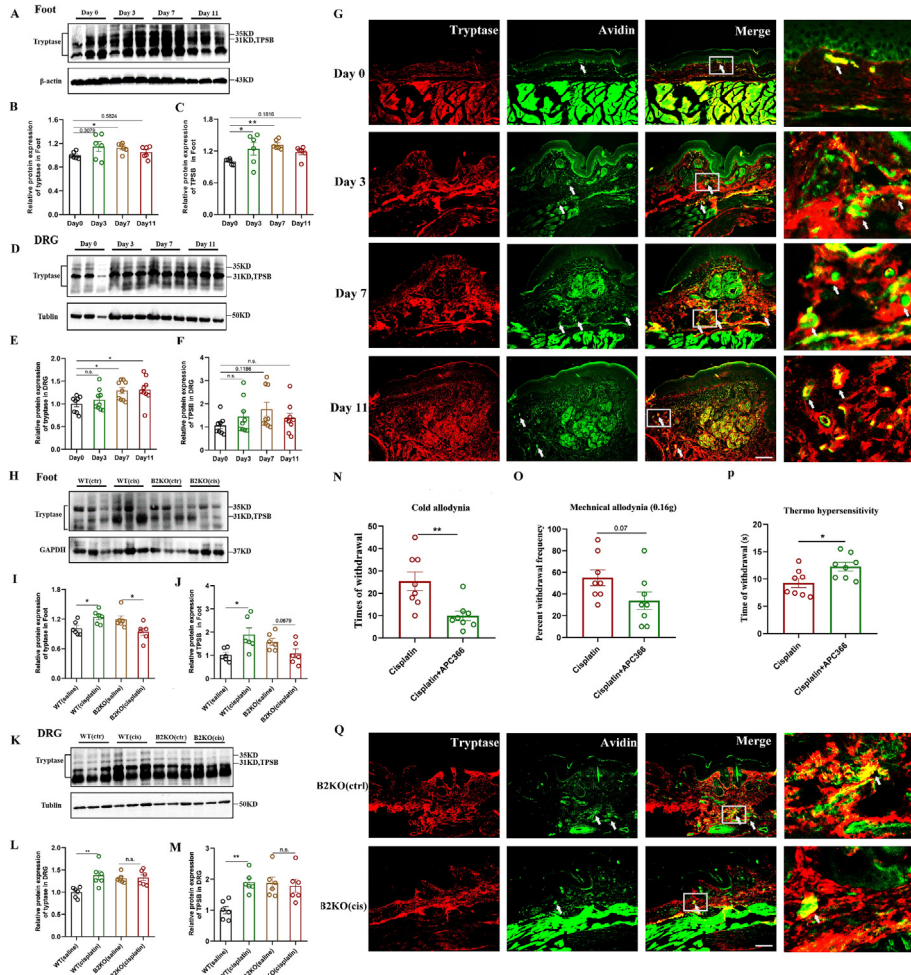


Fig. 2. MrgprB2 participates in cisplatin-induced pain via tryptase. (A-C) Western blot showing an increased tryptase and β -tryptase expression in hindpaw tissues of WT mice after modeling. Data were analyzed using one-way ANOVA with Dunnett's multiple comparisons test, error bars show SEM, $*p < 0.05$, $**p < 0.01$, $n = 6$. (D-F) Western blot showing an increased tryptase and β -tryptase expression in whole DRGs of WT mice after modeling. Data were analyzed using one-way ANOVA with Dunnett's multiple comparisons test, error bars show SEM, $*p < 0.05$, $n = 8$, 9, 9, and 9 for the groups of day 0, 3, 7, and 11, respectively. (G) Immunofluorescence images of hindpaw tissue sections of WT mice at different time points after modeling, arrows point to tryptase-positive cells (red) co-stained with mast cell marker avidin (green). Scale bar was 100 μm . (H-J) Western blot showing no elevated tryptase and β -tryptase expression in hindpaw tissues of MrgprB2^{-/-} mice. Data were analyzed using one-way ANOVA with Dunnett's multiple comparisons test, error bars show SEM, $*p < 0.05$, $n = 6$. (K-M) Western blot showing no elevated tryptase and β -tryptase expression in whole DRGs of MrgprB2^{-/-} mice. Data were analyzed using one-way ANOVA with Dunnett's multiple comparisons test, error bars show SEM, $**p < 0.01$, $n = 6$. (N-P) At day 7, model mice were treated with APC 366 (5 mg/kg) or saline (intraperitoneal injection), and cold allodynia (N), mechanical allodynia (O), and thermal hypersensitivity (P) were measured 1h later. Data were analyzed using two-tailed Student's *t* test, error bars show SEM, $*p < 0.05$, $**p < 0.01$, $n = 8$. (Q) Immunofluorescence images of hindpaw tissue sections of MrgprB2^{-/-} mice after modeling, arrows point to tryptase-positive cells (red) co-stained with mast cell marker avidin (green). Scale bar was 100 μm (125 \times).

Fig. 1. MrgprB2 receptor was involved in cisplatin-induced neuropathic pain. (A-C) Behavioral tests of pain induced by cisplatin. Cold allodynia (A), mechanical allodynia (B) and thermal (C) hypersensitivity were measured at day 0, 3, 7 and 11, respectively. Data were analyzed using one-way ANOVA with Dunnett's multiple comparisons test, error bars show SEM, $*p < 0.05$, $**p < 0.01$, $n = 6$. (D) MrgprB2 mRNA expression in hindpaw tissues of model mice induced by cisplatin. Data were analyzed using one-way ANOVA with Dunnett's multiple comparisons test, error bars show SEM, $*p < 0.05$, $n = 6$. (E) Image of hindpaw (top) and DRG (bottom) sections comparing saline group to model group. MrgprB2 positive mast cells (red) are identified with arrows. Scale bars was 100 μm (125 \times). (F-H) Cisplatin-induced pain was performed on WT or MrgprB2^{-/-} female mice. MrgprB2^{-/-} female mice showed a significant decrease in cold allodynia induced by cisplatin (F), and a partial remission of mechanical allodynia (G) and thermal hypersensitivity (H). Data were analyzed using two-tailed Student's *t* test, error bars show SEM, $*p < 0.05$, $**p < 0.01$, $n = 5$. (I-K) Cisplatin-induced pain was performed on WT or MrgprB2^{-/-} male mice. MrgprB2^{-/-} male mice showed a significant decrease in cold allodynia induced by cisplatin (I), and a partial remission of mechanical allodynia (J) and thermal hypersensitivity (K). Data were analyzed using two-tailed Student's *t* test, error bars show SEM, $*p < 0.05$, $**p < 0.01$, $***p < 0.001$, $n = 5$. (L) Immunofluorescence of Substance P expression in DRG at different time points in cisplatin induced pain. Scale bars was 100 μm (125 \times). (M) Inflammatory cytokines were assessed by the Proteome Profiler Mouse XL Cytokine Array. (N) Substance P concentration was measured at day 7 after cisplatin treatment. Data were analyzed using two-tailed Student's *t* test, error bars show SEM, $*p < 0.05$, $n = 4$. (O) Proportion of SP⁺ neurons were measured at day 0, 3, 7 and 11, respectively. Data were analyzed using one-way ANOVA with Dunnett's multiple comparisons test, error bars show SEM, $*p < 0.05$, $n = 6$, 4, 7, and 5 for the groups of day 0, 3, 7, and 11, respectively. (P-R) At day 7, Anti-SP (2 μg of Anti-SP was dissolved in 20 μL of saline) or mouse IgG (2 μg of IgG was dissolved in 20 μL of saline) were injected into the left and right hindpaws of the model mice, respectively. After 1 h, measurements of cold allodynia (P, unilateral), mechanical allodynia (Q), and thermal hypersensitivity (R) were conducted on the left and right hindpaws, respectively. Data were analyzed using two-tailed Student's *t* test, error bars show SEM, $*p < 0.05$, $n = 4$.

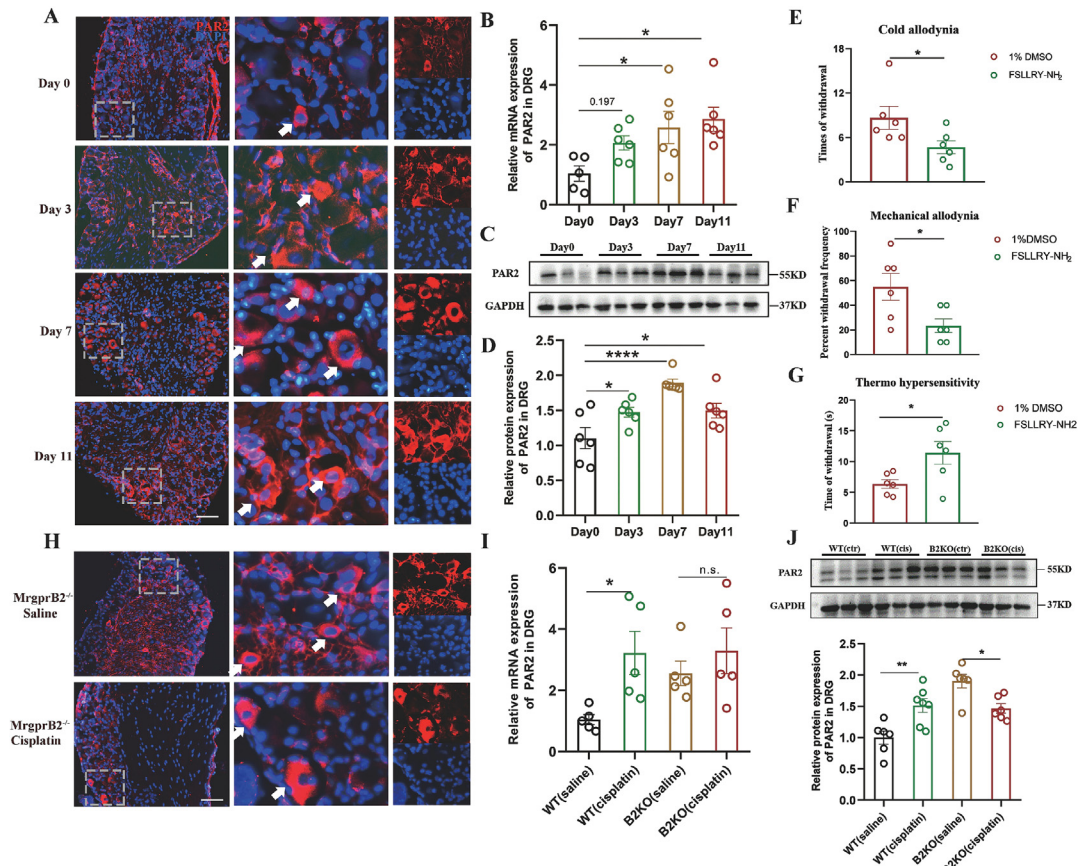


Fig. 3. MrgprB2 participates in cisplatin-induced pain via PAR2. (A-D) PAR2 expression at different time points induced by cisplatin in WT mice. Immunofluorescence (A), the mRNA expression (B), and the protein expression (C, D) of PAR2 in whole DRGs were measured at day 0, 3, 7 and 11, respectively. Scale bars was 100 μ m (200 \times). Data were analyzed using one-way ANOVA with Dunnett's multiple comparisons test, error bars show SEM, * $p < 0.05$, **** $p < 0.0001$, $n = 6$. (E-G) At day 7, FSLRLY-NH₂ (15 μ g) or 1% DMSO were injected into the left and right hindpaws of model mice, respectively. Cold allodynia (E, unilateral), mechanical allodynia (F) and thermal hypersensitivity (G) were measured 1h later. Data were analyzed using two-tailed Student's *t* test, error bars show SEM, * $p < 0.05$, $n = 6$. (H-J) PAR2 expression induced by cisplatin in WT mice and MrgprB2^{-/-} mice. Immunofluorescence (H), the mRNA expression (I), and the protein expression (J) of PAR2 in whole DRGs were measured in WT mice and MrgprB2^{-/-} mice. Data were analyzed using two-tailed Student's *t* test, error bars show SEM, * $p < 0.05$, $n = 5$ for panel I, $n = 6$ for panel J.

protein level in untreated MrgprB2^{-/-} mice (Fig. 5E-F). At the same time, the results of calcium imaging showed that the activity of PAR2 was up-regulated in whole DRGs of untreated MrgprB2^{-/-} mice (Fig. 5G-H). But the activity of MrgprD was not significantly changed (Fig. 5I-J), which may be because β -alanine could not fully reflect the activity of MrgprD in vitro. In addition, injection of the PAR2 agonist SLIGRL-NH₂ into the hindpaw of MrgprB2^{-/-} mice showed significantly increased pain hypersensitivity compared with WT mice (Fig. 5K-L). Meanwhile, we also found the scratching behavior induced by β -alanine was decreased in MrgprB2^{-/-} mice (Fig. 5N). These results demonstrated the negative correlation between PAR2 and MrgprD.

To further confirm this hypothesis, we also investigated the expression of PAR2 in whole DRGs of MrgprD^{-/-} mice. As we expect, untreated MrgprD^{-/-} mice had a significantly increase in PAR2 expression compared with untreated WT mice (Fig. 5M, O-Q). Accordingly, calcium imaging analysis showed that the activity of PAR2 was increased in whole DRGs of MrgprD^{-/-} mice (Fig. 5R-S). We also found that MrgprD^{-/-} mice had an increase in the pain hypersensitivity induced by SLIGRL-NH₂ compared with WT mice (Fig. 5T-U). These findings further pointing to the negative correlation between PAR2 and MrgprD in DRGs.

Furthermore, neurons responding to both β -alanine and SLIGRL-NH₂ stimulation demonstrated a significantly lower response to β -alanine than neurons respond to responding to β -alanine alone (Fig. 5V). At the same time, neurons responding

to both SLIGRL-NH₂ and β -alanine stimulation exhibited a lower response to SLIGRL-NH₂ than neurons responding to SLIGRL-NH₂ alone (Fig. 5W), indicating the mutual inhibition between PAR2 and MrgprD. Single-cell sequencing data also showed that the MrgprD expression in PAR2⁺ neurons was lower to some extent than that in PAR2⁻ neurons; and the PAR2 expression in MrgprD⁺ neurons was lower to some extent than that in MrgprD⁻ neurons, which further confirming the mutual inhibitory relationship between PAR2 and MrgprD (Fig. 5X, Y). Additionally, we observed MrgprD mRNA expression was decreased in isolated DRG neurons induced by SLIGRL-NH₂ stimulation (Fig. S5A), indicating the negative regulatory effect of PAR2 on MrgprD. However, co-immunoprecipitation result showed that there was no obvious direct interaction between PAR2 receptor and MrgprD receptor in DRG (Fig. S5B). Hence, we suggested that the mechanism of the negative correlation between PAR2 and MrgprD in DRG may be indirectly.

PAR2 receptor negatively regulated MrgprD receptor expression in chronic pain

The above results indicated that under physiological conditions, PAR2 could negatively regulate MrgprD. We hypothesized that PAR2 might also negatively regulate MrgprD in pain conditions. Therefore, we subsequently carried out an in-depth exploration in chronic pain models related to MrgprB2 receptor. As

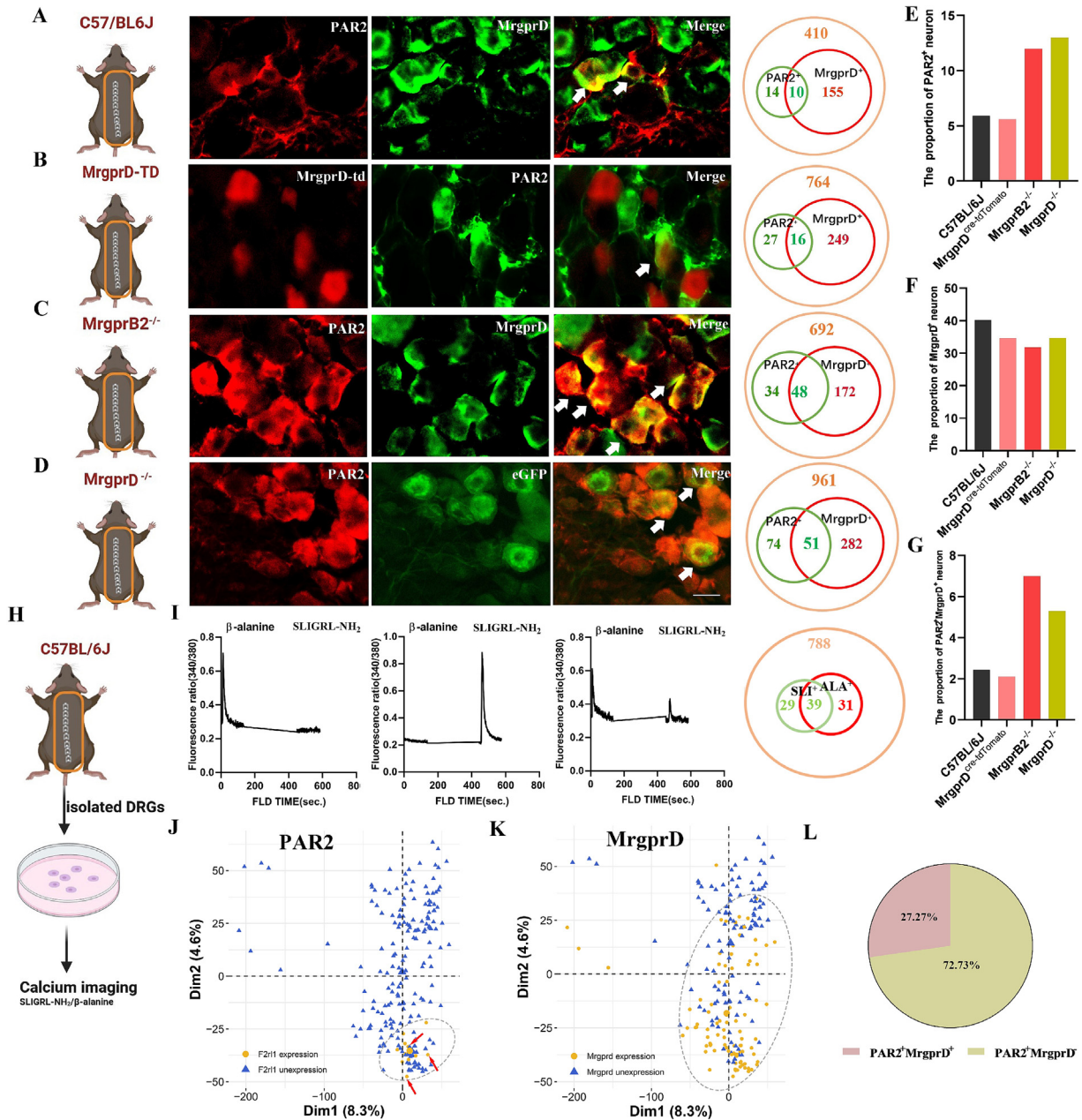


Fig. 4. PAR2 and MrgprD are partially co-expressed in DRG neurons. (A–D) Immunofluorescence images and quantification of DRG sections from WT mice (A), MrgprD-TD mice (B), MrgprB2^{-/-} mice (C), and MrgprD^{-/-} mice (D), co-expressed neurons are identified with arrows. Scale bar was 25 μm. (E–F) Quantification of PAR2⁺ (E), MrgprD⁺ (F), and PAR2⁺MrgprD⁺ (G) DRG neurons in different genotypes of mice. (H, I) Example traces of [Ca²⁺]_i measured by Fura-2 imaging from whole DRG neurons isolated from WT mice exposed to 5 mmol/L β-alanine and 50 μmol/L SLIGRL-NH₂. (J–L) Analysis of single cell sequencing data of DRG neurons in GEO database.

we expect, in cisplatin-induced pain model mice, the expression of MrgprD in DRGs was decreased gradually over time (Fig. 6A–C). Correlation analysis showed that the mRNA expression of PAR2 and MrgprD was significantly negatively correlated at different time points (Fig. 6D), which indicated that PAR2 may be capable of negatively regulating the expression of MrgprD. After long-term treatment with PAR2 inhibitor FSLRLY-NH₂ (4 mg/kg/d for 12 consecutive days) can block the downregulation of MrgprD receptor in CINP (Fig. 6E). These results indicating that downregulation of MrgprD expression induced by cisplatin may be regulated by PAR2. In addition, we also found that the expression of PAR2 was negatively correlated with the expression of MrgprD in postoperative pain (Fig. 6F–I). Similarly, in the CFA pain model, the expression of PAR2 receptor was

up-regulated to a certain extent, and the expression of MrgprD receptor was also decreased to a certain extent, although these changes were not statistically significant (Fig. S6A, B). These results confirmed that PAR2 could regulate MrgprD expression in chronic pain. At the same time, the contralateral DRG of post-operative pain and CFA pain model mice were also examined and analyzed. As Fig. S6C, D showed, the expression of PAR2 receptor was slightly up-regulated and the expression of MrgprD receptor was slightly down-regulated in the contralateral DRGs of the postoperative pain model. Nevertheless, the expression of PAR2 and MrgprD receptor was not significantly changed in the contralateral DRGs of the CFA pain model, which may be due to the slight changes in the expression of these two receptors in the ipsilateral DRGs of CFA model mice.

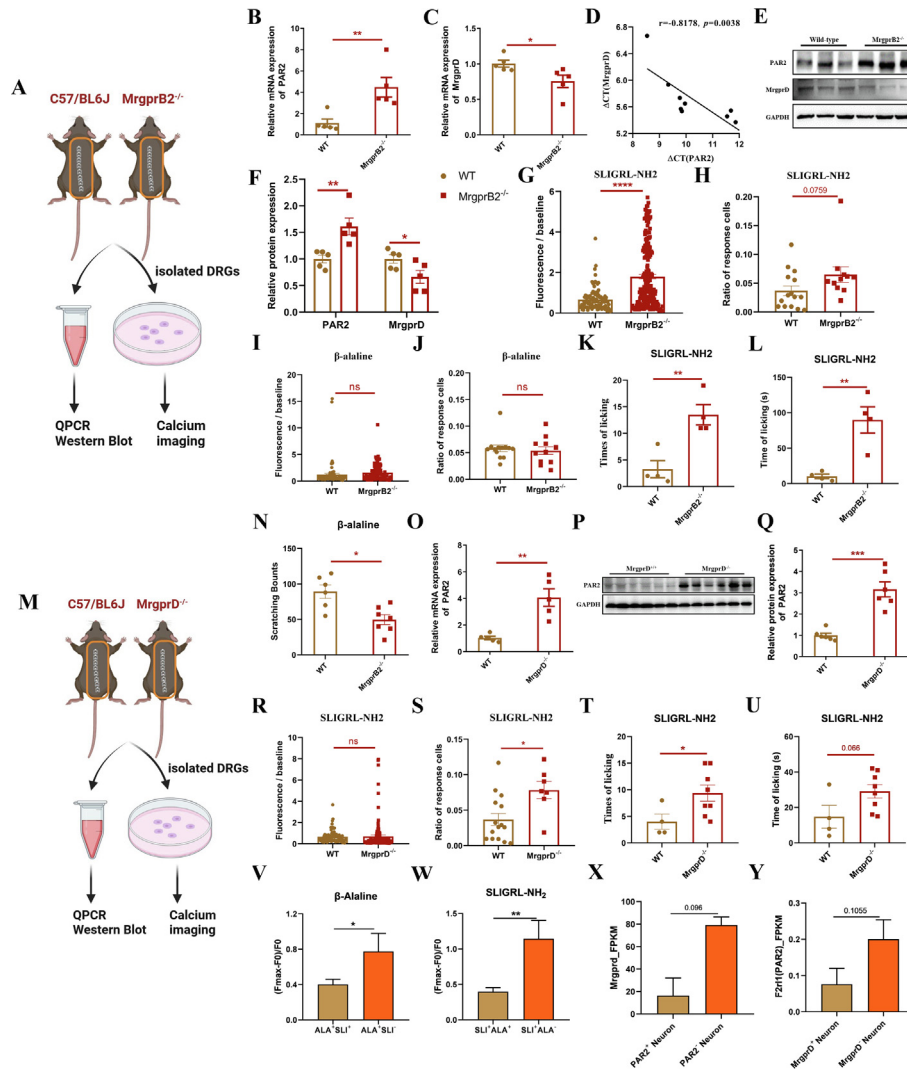
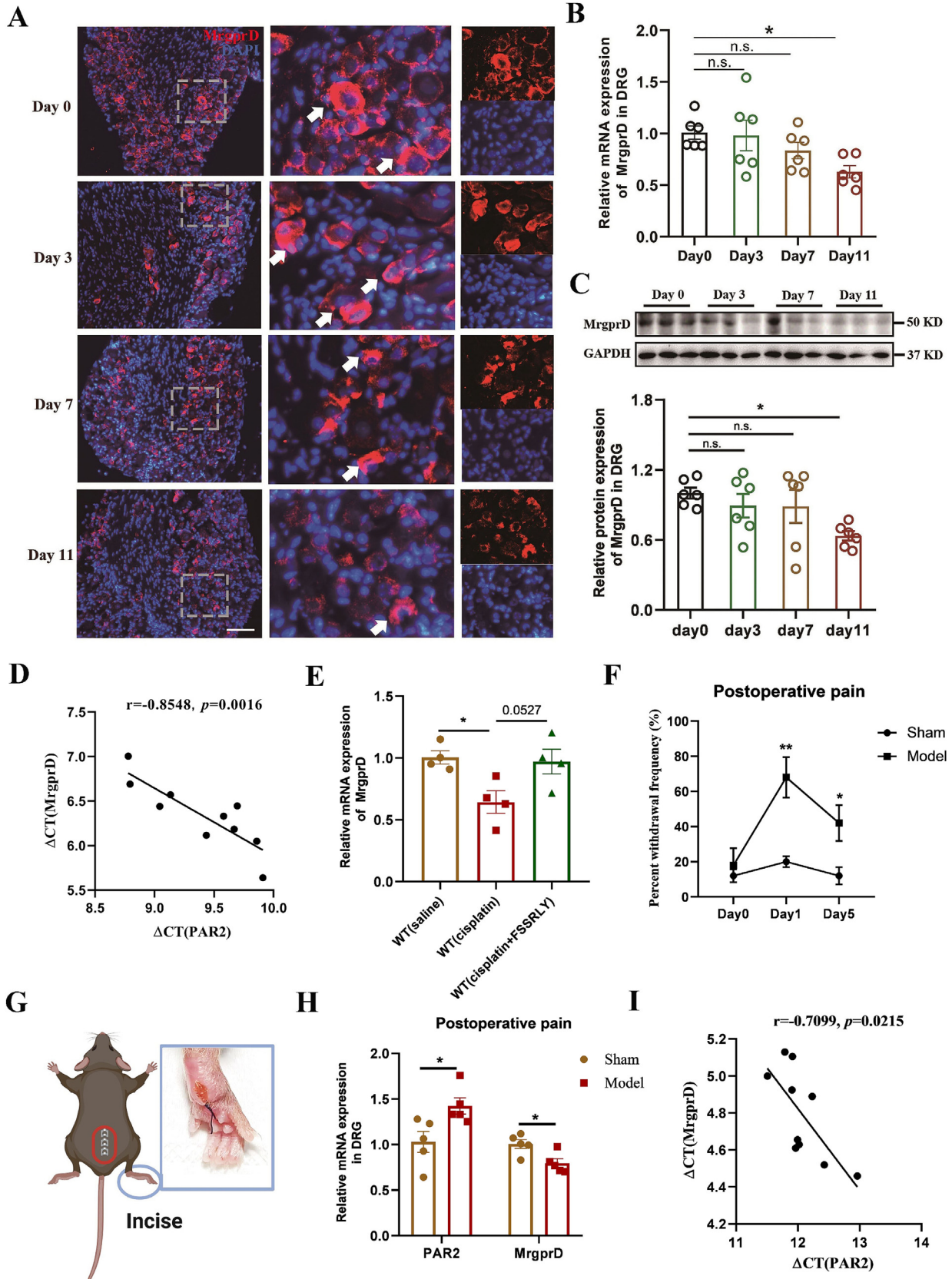


Fig. 5. The negative correlation between PAR2 and MrgprD expression. (A-C) PAR2 mRNA expression (B) and MrgprD mRNA expression (C) in whole DRGs of WT and MrgprB2^{-/-} mice, respectively. Data were analyzed using two-tailed Student's *t* test, error bars show SEM, **p* < 0.05, ***p* < 0.01, n = 5. (D) Correlation analysis between PAR2 mRNA expression and MrgprD mRNA expression. (E, F) The relative protein expression of PAR2 and MrgprD in whole DRGs of WT and MrgprB2^{-/-} mice, respectively. Data were analyzed using two-tailed Student's *t* test, error bars show SEM, **p* < 0.05, ***p* < 0.01, n = 5. (G, H) Quantification of Fluo-4 fluorescence intensity ratio (G) and responding DRG neurons (H) induced by SLIGRL-NH₂ (final concentration was 25 μmol/L) in DRG of WT and MrgprB2^{-/-} mice, respectively. Data were analyzed using two-tailed Student's *t* test, error bars show SEM, *****p* < 0.0001; for panel G, n = 94 and 198 in WT and MrgprB2^{-/-} group, respectively; for panel H, n = 15 and 11 in WT and MrgprB2^{-/-} group, respectively. (I, J) Quantification of Fluo-4 fluorescence intensity ratio (I) and responding DRG neurons (J) induced by β-alanine (final concentration was 2 mmol/L) in DRG of WT and MrgprB2^{-/-} mice, respectively. Data were analyzed using two-tailed Student's *t* test, error bars show SEM; for panel I, n = 77 and 99 in WT and MrgprB2^{-/-} group, respectively; for panel J, n = 13 and 12 in WT and MrgprB2^{-/-} group, respectively. (K, L) The times of licking (K) and the time of licking (L) induced by SLIGRL-NH₂ (100 μmol/L, 1 μL in 25 μL saline, subcutaneous injection) in WT and MrgprB2^{-/-} mice, respectively. Data were analyzed using two-tailed Student's *t* test, error bars show SEM, ***p* < 0.01, n = 4. (N) The scratching bounts induced by β-alanine (100 mmol/L, 1 μL in 50 μL saline, intradermal injection) in WT and MrgprB2^{-/-} mice, respectively. Data were analyzed using two-tailed Student's *t* test, error bars show SEM, **p* < 0.05, n = 6, 7 in WT and MrgprB2^{-/-} group, respectively. (M, O) PAR2 mRNA expression in DRG of WT and MrgprD^{-/-} mice, respectively. Data were analyzed using two-tailed Student's *t* test, error bars show SEM, ***p* < 0.01, n = 5. (P, Q) The relative protein expression of PAR2 in DRG of WT and MrgprD^{-/-} mice, respectively. Data were analyzed using two-tailed Student's *t* test, error bars show SEM, ****p* < 0.001, n = 6. (R, S) Quantification of Fluo-4 fluorescence intensity (R) and responding DRG neurons (S) induced by SLIGRL-NH₂ (final concentration was 25 μmol/L) in DRG of WT and MrgprD^{-/-} mice, respectively (the data of the WT group was shared for panel G, H). Data were analyzed using two-tailed Student's *t* test, error bars show SEM, **p* < 0.05; for panel R, n = 94 and 113 in WT and MrgprD^{-/-} group, respectively; for panel S, n = 15 and 7 in WT and MrgprD^{-/-} group, respectively. (T, U) The times of licking (T) and the time of licking (U) induced by SLIGRL-NH₂ (100 μmol/L, 1 μL in 25 μL saline, subcutaneous injection) in WT and MrgprD^{-/-} mice, respectively. Data were analyzed using two-tailed Student's *t* test, error bars show SEM, **p* < 0.05, n = 4, 8 in WT and MrgprD^{-/-} group, respectively. (V) Quantification of Fura-2 fluorescence intensity ratio induced by β-alanine (5 mmol/L) in ALA⁺SLI⁺ neurons and ALA⁺SLI⁻ neurons, respectively. Data were analyzed using two-tailed Student's *t* test, error bars show SEM. **p* < 0.05, ***p* < 0.01, n = 39 and 31 for ALA⁺SLI⁺ neurons and ALA⁺SLI⁻ neurons, respectively. (W) Quantification of Fura-2 fluorescence intensity ratio induced by SLIGRL-NH₂ (50 μmol/L) in SLI⁺ALA⁺ neurons and SLI⁺ALA⁻ neurons, respectively. Data were analyzed using two-tailed Student's *t* test, error bars show SEM. n = 39 and 29 for ALA⁺SLI⁺ neurons and ALA⁺SLI⁻ neurons, respectively. (X, Y) Mining and analysis of single-cell sequencing databases (GSE155622 and GSE63576). (X) The differential expression of MrgprD in PAR2⁺ neurons and PAR2⁻ neurons. (Y) The differential expression of PAR2 in MrgprD⁺ neurons and MrgprD⁻ neurons. Data were analyzed using two-tailed Student's *t* test, error bars show SEM, for panel X, n = 18, 483; for panel Y, n = 187, 314.

MrgprB2 receptor-dependent neural immune axis is implicated in pain resolution through down-regulating MrgprD receptor

The above results indicated that PAR2 could downregulate the expression of MrgprD in the later stage of cisplatin-induced pain,

which is a common phenomenon. MrgprD receptor has also been reported to be downregulated in several chronic diseases, such as psoriasis [32], and spared nerve injury [26]. Next, we investigated the potential impact of MrgprD downregulation on cisplatin-induced pain. Compared to WT mice, MrgprD^{-/-} mice had reduced



tions in both cold and mechanical allodynia, but not decreased thermal hypersensitivity (Fig. 7A-C). In addition, MrgprD^{-/-} mice also partially alleviated cisplatin-induced weight loss (Fig. S2D). These findings suggested that MrgprD receptor was involved in the development of cisplatin-induced pain. Therefore, the downregulation of MrgprD expression could contribute to the alleviation of cisplatin-induced pain. This was consistent with the findings that pain behavior did not consistently increase over time despite daily cisplatin stimulation (Fig. 1A-C). Furthermore, long-term inhibition of PAR2 activity with FSLLRY-NH₂ could significantly alleviate cisplatin-induced pain in the early stage; however, it did not exhibit a notable analgesic effect in the later stages (Fig. 7D-F). This may be attributed to the blockade of MrgprD downregulation caused by prolonged inhibition of PAR2 (Fig. 6E). These findings further indicated that PAR2 was involved in pain resolution by negatively regulating the expression of MrgprD. Given that MrgprB2 can mediate the activation of the Tryptase/PAR2 axis, we hypothesized that MrgprB2 activation could result in MrgprD downregulation. As Fig. 7G-J showed, substance P or PAMP-12 treatment could significantly decrease the MrgprD expression in DRGs, which could be blocked by MrgprB2 knockout (Fig. S7). These results indicated that the negative regulatory role of the MrgprB2 receptor on MrgprD expression. Moreover, we also found that MrgprB2 mRNA expression was negatively correlated with MrgprD mRNA expression in cisplatin-induced pain (Fig. 7K). Knocking out of MrgprB2 receptor could effectively block the downregulation of MrgprD in the CINP model (Fig. 7L), which further confirmed that MrgprB2 activation could negatively affect the expression of MrgprD. Taken together, we proposed that the MrgprB2/Tryptase/PAR2 axis also contributed to pain resolution by downregulating MrgprD expression in the later stages of CINP. This was in line with the findings that pain behavior in mice was in dynamic equilibrium at the later stage despite daily cisplatin stimulation.

Discussion

Here we elucidated a novel pain modulation mechanism involving neuron-mast cell interactions, specifically highlighting the bidirectional modulation of MrgprB2-dependent neural immune axis in CINP. The Substance P/MrgprB2/Tryptase/PAR2 axis not only participated in the mechanism of pain hypersensitivity, but also alleviated the pain perception by downregulating MrgprD expression in the later stage of CINP.

The neuro-immune interactions play important roles in the peripheral and central sensitization processes of chronic pain, which has been widely recognized. For instance, immune cells such as macrophages, neutrophils, and mast cells can directly or indirectly enhance the excitability of peripheral nociceptive neurons [33]. It is well established that neuro-immune interaction is a potential common driver of CINP. Activation of mast cells has been shown to play an important role in neuropathic pain induced by chemotherapeutic drugs such as vincristine, oxaliplatin, and

paclitaxel [8–10]. In our current study, the results demonstrated that MrgprB2/Tryptase/PAR2 axis played a crucial role in cisplatin-induced allodynia. MrgprB2^{-/-} mice significantly attenuated cisplatin-induced cold hypersensitivity and partially reduced the mechanical and thermal hypersensitivity. Similar to the study on postoperative pain model [14], MrgprB2^{-/-} mice could also inhibit cisplatin-induced inflammatory cells infiltration, which may also be related to the activation of MrgprB2 by substance P in model mice. However, Sash mice could not alleviate the mechanical and thermal pain induced by cisplatin. The possible reason is the abnormal immune cell populations caused by Kit^{W^{-SH}}, such as the increase of the medium and high expression populations of Ly6G in spleen of Sash mice [34]. In addition, we observed that deletion of mast cells or MrgprB2 receptor did not alleviate cisplatin-induced weight loss, suggesting that unlike NK1R, the classical receptor for substance P, MrgprB2 receptor may not be involved in cisplatin-induced digestive responses such as nausea and vomiting.

Notably, emerging research evidence indicates that neuro-immune interactions play crucial roles in pain relief. Some immune cells are capable of producing various pro-resolution or anti-inflammatory mediators, which subsequently reduce the excitability of sensory neurons and alleviate pain [35]. Several studies have shown that immune cells such as Treg [36] or CD11c⁺ spinal microglia populations [37] are essential for pain recovery. In addition, neutrophils cells can secrete pain-relieving mediators such as opioid peptides to alleviate pain [38], and can also promote pain relief by inhibiting T cell responses through the macrophage antigen-1 (Mac-1) [39]. Furthermore, macrophages can also play important roles in alleviating chronic pain. Research indicates that M2 macrophages can mitigate pain by releasing IL-4 and IL-10 [40]. Also, studies have shown that M2 macrophages could transfer mitochondria to DRG neurons, thereby reducing the excitability of neurons and contributing to pain relief [41]. Despite this, the neuron-mast cell interactions in pain relief have not been thoroughly investigated.

Interestingly, our findings also revealed that MrgprB2 receptor was involved in pain alleviation during the later stages of the CINP model through the downregulation of MrgprD expression. MrgprD-expressing neurons mainly innervate the skin and can be activated by chemical, mechanical, and thermal stimuli [42]. It is well known that MrgprD is implicated in pain hypersensitivity, such as CFA inflammatory pain [23] and CCI-neuropathic pain [25]. Our findings demonstrated that knocking out MrgprD could alleviate cisplatin-induced pain, suggesting that MrgprD also contributed to the progression of CINP. Therefore, the downregulation of MrgprD resulting from the activation of MrgprB2 could contribute to alleviating cisplatin-induced pain. In the CINP model, MrgprD expression decreased gradually over time and presented a significant downregulation in the later stages. However, during the early stage of the CINP model, MrgprD expression was not significantly down-regulated. This might be due to the fact that the activation of MrgprB2 at the early stage was not sufficient to cause

Fig. 6. PAR2 receptor negatively regulated MrgprD receptor expression in chronic pain. (A-C) MrgprD expression at different time points in this model. Immunofluorescence (A), the mRNA expression (B), and the protein expression (C) of MrgprD in whole DRGs were measured at day 0, 3, 7 and 11, respectively. Scale bars was 100 μm (125×). Data were analyzed using one-way ANOVA with Dunnett's multiple comparisons test, error bars show SEM, **p* < 0.05, *n* = 6. (D) Correlation analysis between PAR2 mRNA expression (ΔCT) and MrgprD mRNA expression (ΔCT) in DRG of model mice at different time points. (E) Long-term treatment with PAR2 inhibitor FSLLRY-NH₂ (4 mg/kg/d from day 0 to day 11, i.p.) blocked the downregulation of MrgprD receptor induced by cisplatin. Data were analyzed using one-way ANOVA with Dunnett's multiple comparisons test, error bars show SEM, **p* < 0.05, *n* = 4. (F, G) Behavioral tests of mechanical allodynia in postoperative pain model. Data were analyzed using two-tailed Student's *t* test, error bars show SEM, **p* < 0.05, ***p* < 0.01, *n* = 5. (H) The mRNA expression of PAR2 and MrgprD in whole DRGs of postoperative pain model at day 5. Data were analyzed using two-tailed Student's *t* test, error bars show SEM, **p* < 0.05, *n* = 5. (I) Correlation analysis between PAR2 mRNA expression (ΔCT) and MrgprD mRNA expression (ΔCT) in DRG of postoperative pain model.

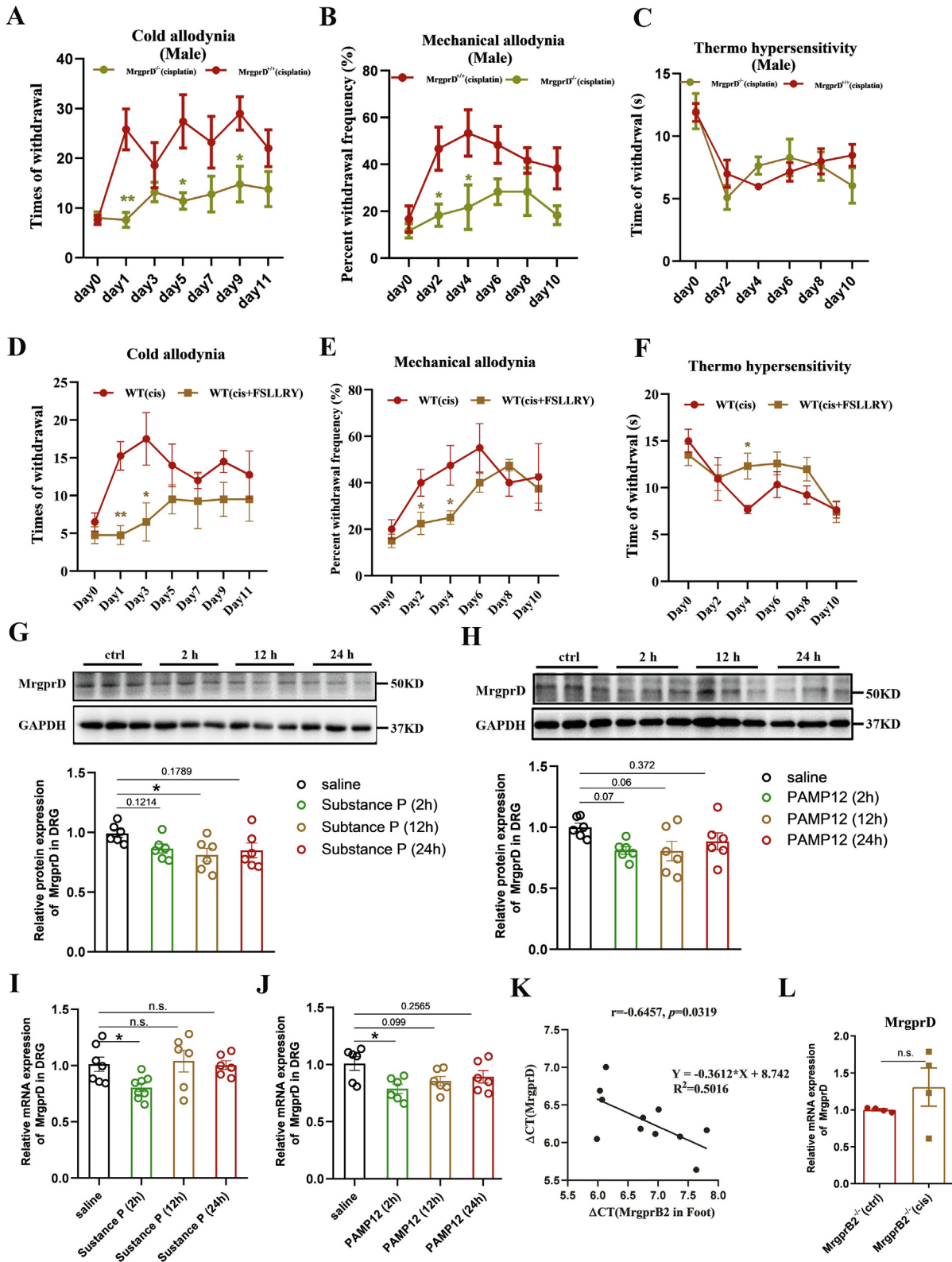


Fig. 7. MrgprB2 receptor-dependent neural immune axis is implicated in pain resolution through down-regulating MrgprD receptor. (A-C) Cisplatin-induced pain was performed on WT or MrgprD^{-/-} mice. MrgprD^{-/-} male mice showed reductions in cold (A) and mechanical allodynia (B), but not in thermal hypersensitivity (C). Data were analyzed using two-tailed Student's *t* test, error bars show SEM, **p* < 0.05, ***p* < 0.01, *n* = 5. (D-F) Effects of long-term treatment with PAR2 inhibitor FSLRY-NH₂ (4 mg/kg/d from day 0 to day 11, i.p., and behavioral tests were performed 1 h after FSLRY-NH₂ treatment) on cold allodynia (D, unilateral), mechanical allodynia (E), thermal hypersensitivity (F) induced by cisplatin cold. Data were analyzed using two-tailed Student's *t* test, error bars show SEM, **p* < 0.05, ***p* < 0.01, *n* = 4. (G-J) Effects of MrgprB2 agonists substance P or PAMP-12 on MrgprD expression. Substance P (10 μg per mice, intradermal injection) treatment could significantly inhibited the mRNA (I) and the protein (G) expression of MrgprD in DRGs. PAMP-12 (40 μg per mice, intradermal injection) treatment could significantly inhibited the mRNA (J) and the protein (H) expression of MrgprD in DRGs. Data were analyzed using one-way ANOVA with Dunnett's multiple comparisons test, error bars show SEM, **p* < 0.05, ***p* < 0.01, *n* = 6–8. (K) Correlation analysis between MrgprB2 mRNA expression (ΔCT) in hindpaw tissues and MrgprD mRNA expression (ΔCT) in whole DRGs of model mice at different time points. (L) MrgprD mRNA expression changes in whole DRGs of MrgprB2^{-/-} mice induced by cisplatin. Data were analyzed using two-tailed Student's *t* test, error bars show SEM, *n* = 4.

a significant downregulation of MrgprD. Therefore, results indicated that the role of MrgprB2 receptor in pain relief mainly emerged in the late stages of CINP, which was consistent with the findings that pain behavior remained in dynamic equilibrium in the later stage under continuous cisplatin stimulation.

The present study further elucidated that the mechanism by which MrgprB2 activation down-regulated the MrgprD expression was related to PAR2 receptor. Studies have shown that PAR2 and Mrgprs are partially co-expressed in DRG neurons, and that activation of PAR2 can regulate the function of Mrgprs [21]. Our results indicated that PAR2 and MrgprD are partially co-expressed. Immunofluorescence results showed that approximately 40 % of the PAR2-positive neurons in wild-type mice expressed the MrgprD receptor, and the single-cell sequencing data also revealed that about 30 % of the PAR2-positive neurons expressed the MrgprD receptor. Under physiological conditions, the expression levels of PAR2 receptor and MrgprD receptor were negatively correlated in DRGs; and the activation of the PAR2 receptor could down-regulate the expression of MrgprD receptor. Meanwhile, in pathological conditions such as CINP model, the activation of PAR2 could also suppress the expression of MrgprD. Long-term inhibition of PAR2 activity could block the downregulation of MrgprD expression and disrupt the pain relief pathway, and subsequently weaken its analgesic effects in the later stages of the CINP model.

In addition to CINP, we also studied the postoperative pain model and CFA model in which MrgprB2 were involved [14]. The results showed that the expression of PAR2 was also negatively correlated with MrgprD expression in postoperative pain, suggesting that the bidirectional modulation of MrgprB2-dependent neural immune axis may also exist in postoperative pain. In summary, the similarity of these three pain models we used was that both substance P and MrgprB2 receptor were involved, but they were also different. For example, in postoperative pain and CFA pain model, chemokines released by MrgprB2 receptor activated by substance P were mainly CCL2 and CCL3. The chemokines released in cisplatin-induced neuropathic pain were mainly CCL3/4, CXCL1, CXCL9, CXCL10, CXCL11, and CXCL13.

Although inhibition of MrgprD has been reported to increase MrgprB2 expression [43], our results showed that MrgprD^{-/-} mice could reduce cisplatin-induced neuropathic pain. This does not mean that these results are contradictory. We found that deletion of MrgprD could prevent cisplatin-induced up-regulation of MrgprB2 expression and the downstream tryptase-PAR2 pathway (Fig. S8). Therefore, we speculated that MrgprD^{-/-} mice may inhibit MrgprB2 upregulation through other pathways, such as the TRP channels [25], inflammation [24], and so on, which need to be further studied.

There are also some limitations in our study. Firstly, our experimental results showed that the expression of MrgprB2 and MrgprD were negatively correlated, and the activation of MrgprB2 could down-regulate MrgprD expression. However, MrgprD expression was found to be reduced in MrgprB2^{-/-} mice, which may be related to other regulatory pathways triggered by global deletion of MrgprB2, such as the increased expression of PAR2. Therefore, the MrgprB2 time-specific gene knockout mice and the MrgprB2 overexpression mice should be applied in the further study. Secondly, although we have demonstrated partial co-expression of the PAR2 receptor and MrgprD receptor in DRG neurons, the results of the ColP experiment indicated no significant direct interaction between these two receptors. Additionally, among all the DRG neurons, the proportion of neurons co-expressing PAR2 and MrgprD was relatively low. Therefore, we suggested that the mutual inhibitory relationship between PAR2 and MrgprD may be indirect, which need to be further studied. Thirdly, our study was limited to animal models, so there is certain

limitation in clinical applicability. In the subsequent studies, further validation is needed in human subjects.

Taken together, results demonstrated that MrgprB2 receptor-dependent neural immune axis not only promoted hyperalgesia induced by cisplatin, but also contributed to the pain recovery at the later stage by down-regulating MrgprD expression. This study indicates that MrgprB2 receptor is a crucial target for early intervention in CINP. It also implies that the treatment of chronic pain requires consideration of the mechanistic differences at various stages. For instance, therapeutic approaches such as the inhibition of MrgprB2 receptor, tryptase, or PAR2 receptor might yield significant pain alleviation effects in the early stage of these pain models. Nevertheless, these treatments may potentially lead to an aberration of pain inhibitory modulation at a later stage, such as the blockade of the downregulation of MrgprD expression, thereby diminishing the analgesic effect.

Conclusions

Our research findings revealed the dual role of the neuron-mast cell interactions in chronic pain. The activation of mast cells mediated by MrgprB2 receptor played crucial roles in both pain sensitization and pain resolution in the CINP model. This study emphasizes that MrgprB2 is a critical target for early intervention in CINP, and highlights the necessity of considering the mechanism differences at different stages in pain management.

Data sharing statement

All data generated for this study are available from the corresponding authors upon reasonable request.

Compliance with ethics requirements

All Institutional and National Guidelines for the care and use of animals were followed.

Declaration of competing interest

The authors declare that they have no known competing financial interests or personal relationships that could have appeared to influence the work reported in this paper.

Acknowledgments

The authors thank Prof. Dong in Johns Hopkins for kindly providing the MrgprB2^{-/-}, MrgprB2-Cre, MrgprD^{-/-}, MrgprD-cre, Kit (W-sh/W-sh), and Isl1-Tdtomato animals. This work was supported by the Project of National Natural Science Foundation of China (No.31771163; No.62074082; No.82404886) and the key project of science and technology development plan of traditional Chinese medicine in Jiangsu Province (No. ZD202001). This work was supported by the Open Project of Chinese Materia Medica First-Class Discipline of Nanjing University of Chinese Medicine (No. 026062024001) and the Innovation Projects of State Key Laboratory on Technologies for Chinese Medicine Pharmaceutical Process Control and Intelligent Manufacture (No. NZYSKL240105).

Author contributions

Conceptualization, Y.J., G.Y., and Z.T.; methodology, Y.J., F.Y., and Z.T.; investigation, Y.J., F.Y., J.Z., Y.H., Y.Z., F.C., Y.Y., C.Z., T.Y., G.Y., and Z.T.; formal analysis, Y.J., and F.Y.; writing – original draft, Y. J.; writing – review & editing, G.Y., and Z.T.; funding acquisition, Y.J., T.Y. and Z.T.; supervision, G.Y., and Z.T.

Appendix A. Supplementary data

Supplementary data to this article can be found online at <https://doi.org/10.1016/j.jare.2025.02.037>.

References

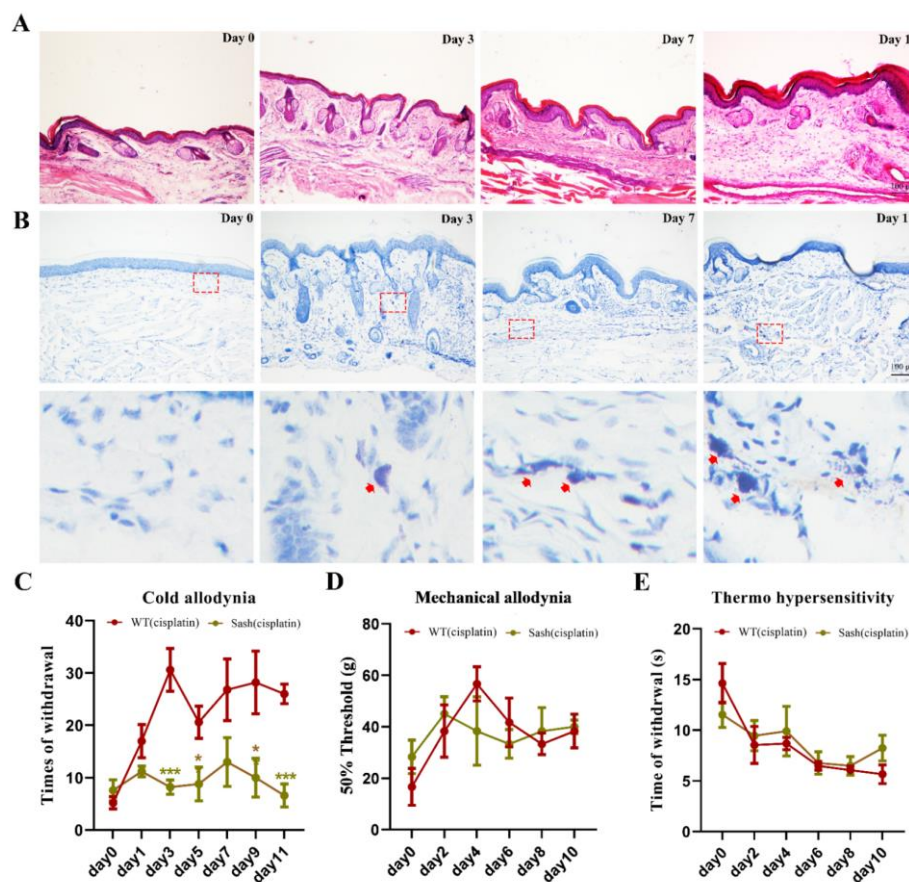
- [1] Ossipov MH, Morimura K, Porreca F. Descending pain modulation and chronification of pain. *Curr Opin Support Palliat Care* 2014;8(2):143–51.
- [2] Luo H, Liu HZ, Zhang WW, Matsuda M, Lv N, Chen G, et al. Interleukin-17 Regulates Neuron-Glial Communications, Synaptic Transmission, and Neuropathic Pain after Chemotherapy. *Cell Rep* 2019;29(8):2384–97.
- [3] Tender T, Rahangdale RR, Balireddy S, Nampoothiri M, Sharma KK, Raghu CH. Melittin, a honeybee venom derived peptide for the treatment of chemotherapy-induced peripheral neuropathy. *Med Oncol* 2021;38(5):52.
- [4] Calls A, Torres-Espin A, Navarro X, Yuste VJ, Udina E, Bruna J. Cisplatin-induced peripheral neuropathy is associated with neuronal senescence-like response. *Neuro Oncol* 2021;23(1):88–99.
- [5] Staff NP, Cavaletti G, Islam B, Lustberg M, Psimaras D, Tamburin S. Platinum-induced peripheral neurotoxicity: From pathogenesis to treatment. *J Peripher Nerv Syst* 2019;Suppl 2(Suppl 2):S26–39.
- [6] Loprinzi CL, Lacchetti C, Bleeker J, Cavaletti G, Chauhan C, Hertz DL, et al. Prevention and Management of Chemotherapy-Induced Peripheral Neuropathy in Survivors of Adult Cancers: ASCO Guideline Update. *J Clin Oncol* 2020;38(28):3325–48.
- [7] Brandolini L, d'Angelo M, Antonosante A, Allegretti M, Cimini A. Chemokine Signaling in Chemotherapy-Induced Neuropathic Pain. *Int J Mol Sci* 2019;20(12):2904.
- [8] Jaggi AS, Kaur G, Bali A, Singh N. Pharmacological investigations on mast cell stabilizer and histamine receptor antagonists in vincristine-induced neuropathic pain. *Naunyn Schmiedeberg's Arch Pharmacol* 2017;390(11):1087–96.
- [9] Sakamoto A, Andoh T, Kuraishi Y. Involvement of mast cells and proteinase-activated receptor 2 in oxaliplatin-induced mechanical allodynia in mice. *Pharmacol Res* 2016;105:84–92.
- [10] Chen Y, Yang C, Wang ZJ. Proteinase-activated receptor 2 sensitizes transient receptor potential vanilloid 1, transient receptor potential vanilloid 4, and transient receptor potential ankyrin 1 in paclitaxel-induced neuropathic pain. *Neuroscience* 2011;193:440–51.
- [11] Fiore NT, Debs SR, Hayes JP, Duffy SS, Moalem-Taylor G. Pain-resolving immune mechanisms in neuropathic pain. *Nat Rev Neurol* 2023;19(4):199–220.
- [12] Meixiong J, Dong X. Mas-Related G Protein-Coupled Receptors and the Biology of Itch Sensation. *Annu Rev Genet* 2017;51:103–21.
- [13] Roy S, Chompunud Na Ayudhya C, Thapaliya M, Deepak V, Ali H. Multifaceted MRGPRX2: New insight into the role of mast cells in health and disease. *J Allergy Clin Immunol* 2021;148(2):293–308.
- [14] Green DP, Limjunyawong N, Gour N, Pundir P, Dong XZ. A Mast-Cell-Specific Receptor Mediates Neurogenic Inflammation and Pain. *Neuron* 2019;101(3):412–20.
- [15] Son H, Zhang Y, Shannonhouse J, Ishida H, Gomez R, Kim YS. Mast-cell-specific receptor mediates alcohol-withdrawal-associated headache in male mice. *Neuron* 2024;112(1):113–123.e4.
- [16] Sbei S, Moncrief T, Limjunyawong N, Zeng Y, Green DP. PACAP activates MRGPRX2 on meningeal mast cells to drive migraine-like pain. *Sci Rep* 2023;13(1):12302.
- [17] Meixiong J, Anderson M, Limjunyawong N, Sabbagh MF, Hu E, Mack MR, et al. Activation of Mast-Cell-Expressed Mas-Related G-Protein-Coupled Receptors Drives Non-histaminergic Itch. *Immunity* 2019;50(5):1163–1171.e5.
- [18] Mrozkova P, Palecek J, Spicarova D. The role of protease-activated receptor type 2 in nociceptive signaling and pain. *Physiol Res* 2016;65(3):357–67.
- [19] Wang Q, Wang J, Gao D, Li J. Inhibition of PAR2 and TRPA1 signals alleviates neuropathic pain evoked by chemotherapeutic bortezomib. *J Biol Regul Homeost Agents* 2017;31(4):977–83.
- [20] Chen K, Zhang ZF, Liao MF, Yao WL, Wang J, Wang XR. Blocking PAR2 attenuates oxaliplatin-induced neuropathic pain via TRPV1 and releases of substance P and CGRP in superficial dorsal horn of spinal cord. *J Neurol Sci* 2015;352(1–2):62–7.
- [21] Akiyama T, Tominaga M, Davoodi A, Nagamine M, Blansit K, Horwitz A, et al. Cross-sensitization of histamine-independent itch in mouse primary sensory neurons. *Neuroscience* 2012;226:305–12.
- [22] Dong X, Han S, Zylka MJ, Simon MI, Anderson DJ. A diverse family of GPCRs expressed in specific subsets of nociceptive sensory neurons. *Cell* 2001;106(5):619–32.
- [23] Cavanaugh DJ, Lee H, Lo L, Shields SD, Zylka MJ, Basbaum AI, et al. Distinct subsets of unmyelinated primary sensory fibers mediate behavioral responses to noxious thermal and mechanical stimuli. *Proc Natl Acad Sci U S A* 2009;106(22):9075–80.
- [24] Lan L, Xu M, Li J, Liu L, Xu M, Zhou CX, et al. Mas-related G protein-coupled receptor D participates in inflammatory pain by promoting NF-κB activation through interaction with TAK1 and IKK complex. *Cell Signal* 2020;76:109813.
- [25] Wang CM, Gu LY, Ruan YL, Geng X, Xu M, Yang NN, et al. Facilitation of MrgprD by TRP-A1 promotes neuropathic pain. *FASEB J* 2019;33(1):1360–73.
- [26] Wang KK, Wang SS, Chen Y, Wu D, Hu XY, Lu YJ, et al. Single-cell transcriptomic analysis of somatosensory neurons uncovers temporal development of neuropathic pain. *Cell Res* 2021;31(8):904–18.
- [27] Khasabova IA, Khasabov S, Paz J, Harding-Rose C, Simone DA, Seybold VS. Cannabinoid type-1 receptor reduces pain and neurotoxicity produced by chemotherapy. *J Neurosci* 2012;32(20):7091–101.
- [28] Jiang YC, Ye F, Du Y, Zong YX, Tang ZX. P2X7R in Mast Cells is a Potential Target for Salicylic Acid and Aspirin in Treatment of Inflammatory Pain. *J Inflamm Res* 2021;14:2913–31.
- [29] Ruan YL, Gu LY, Yan JJ, Guo J, Geng X, Shi H, et al. An effective and concise device for detecting cold allodynia in mice. *Sci Rep* 2018;8(1):14002.
- [30] He W, Xu JZ, Mu RY, Li Q, Lv DL, Huang Z, et al. High-salt diet inhibits tumour growth in mice via regulating myeloid-derived suppressor cell differentiation. *Nat Commun* 2020;11(1):1732.
- [31] Richards J, Tang S, Gunsch G, Sul P, Wiet M, Flanigan DC, et al. Mast Cell/Proteinase Activated Receptor 2 (PAR2) Mediated Interactions in the Pathogenesis of Discogenic Back Pain. *Front Cell Neurosci* 2019;13:294.
- [32] Sakai K, Sanders KM, Youssef MR, Yanusheski KM, Jensen L, Yospovitch G, et al. Mouse model of imiquimod-induced psoriatic itch. *Pain* 2016;157(11):2536–43.
- [33] Yang JX, Wang HF, Chen JZ, Li HY, Hu JC, Yu AA, et al. Potential Neuroimmune Interaction in Chronic Pain: A Review on Immune Cells in Peripheral and Central Sensitization. *Front Pain Res (Lausanne)* 2022;3:946846.
- [34] Michel A, Schüller A, Friedrich P, Döner F, Bopp T, Radsak M, et al. Mast cell-deficient Kit(W-sh) “Sash” mutant mice display aberrant myelopoiesis leading to the accumulation of splenocytes that act as myeloid-derived suppressor cells. *J Immunol* 2013;190(11):5534–44.
- [35] Zhao J, Huh Y, Bortsov A, Diatchenko L, Ji RR. Immunotherapies in chronic pain through modulation of neuroimmune interactions. *Pharmacol Ther* 2023;248:108476.
- [36] Fischer R, Sendetski M, Del Rivero T, Martinez GF, Bracchi-Ricard V, Swanson KA, et al. TNFR2 promotes Treg-mediated recovery from neuropathic pain across sexes. *Proc Natl Acad Sci U S A* 2019;116(34):17045–50.
- [37] Kohno K, Shirasaka R, Yoshihara K, Mikuriya S, Tanaka K, Takanami K, et al. A spinal microglia population involved in remitting and relapsing neuropathic pain. *Science* 2022;376(6588):86–90.
- [38] Brack A, Rittner HL, Machelka H, Leder K, Mousa SA, Schäfer M, et al. Control of inflammatory pain by chemokine-mediated recruitment of opioid-containing polymorphonuclear cells. *Pain* 2004;112:229–38.
- [39] Pillay J, Kamp VM, van Hoffen E, Visser T, Tak T, Lammers JW, et al. A subset of neutrophils in human systemic inflammation inhibits T cell responses through Mac-1. *J Clin Invest* 2012;122:327–36.
- [40] . *JCI Insight* 2020;5:e133093.
- [41] van der Vlist M, Raouf R, Willemen H, Prado J, Versteeg S, Martin Gil C, et al. Macrophages transfer mitochondria to sensory neurons to resolve inflammatory pain. *Neuron* 2022;110(613–26):e9.
- [42] Guo C, Jiang H, Huang CC, Li F, Olson W, Yang W, et al. Pain and itch coding mechanisms of polymodal sensory neurons. *Cell Rep* 2023;42(11):113316.
- [43] Zhang SQ, Edwards TN, Chaudhri VK, Wu J, Cohen JA, Hirai T, et al. Nonpeptidergic neurons suppress mast cells via glutamate to maintain skin homeostasis. *Cell* 2021;184(8):2151–66.

1 **Supplemental information**

2 **Dual function of MrgprB2 receptor-dependent neural immune**
3 **axis in chronic pain**

4 Yucui Jiang, Fan Ye, Jian Zhang, Yun Huang, Yingxin Zong, Feiyan Chen, Yan Yang, Chan Zhu, Tao
5 Yang, Guang Yu, Zongxiang Tang

6



7

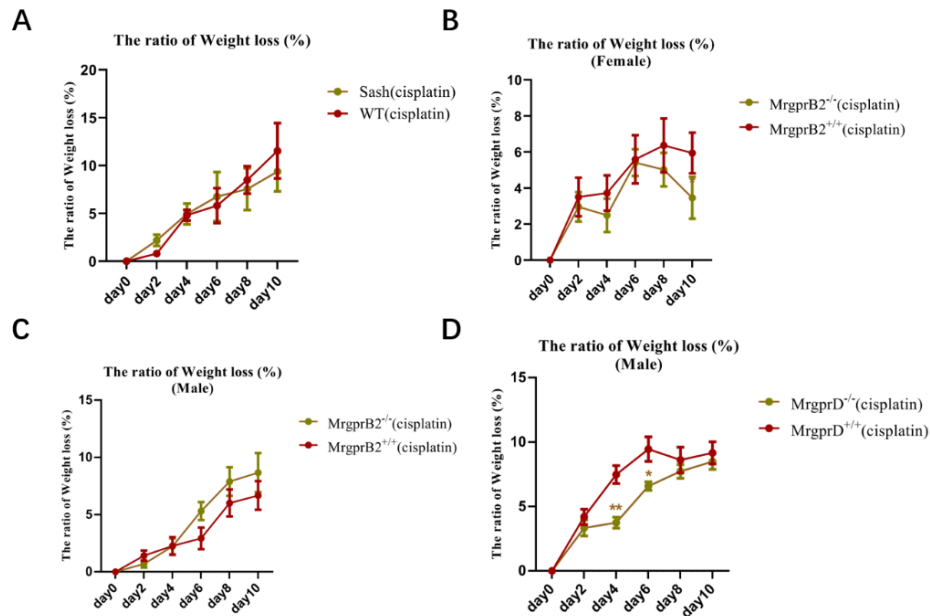
8 **Figure S1** Mast cell-deficient mice alleviated cisplatin-induced neuropathic pain. (A-B)

9 Pathological analysis of paw tissue in cisplatin-induced pain model mice. Samples of the model
10 were analyzed by Hematoxylin-Eosin staining (A) and Toluidine blue staining (B) at day 0, 3, 7 and

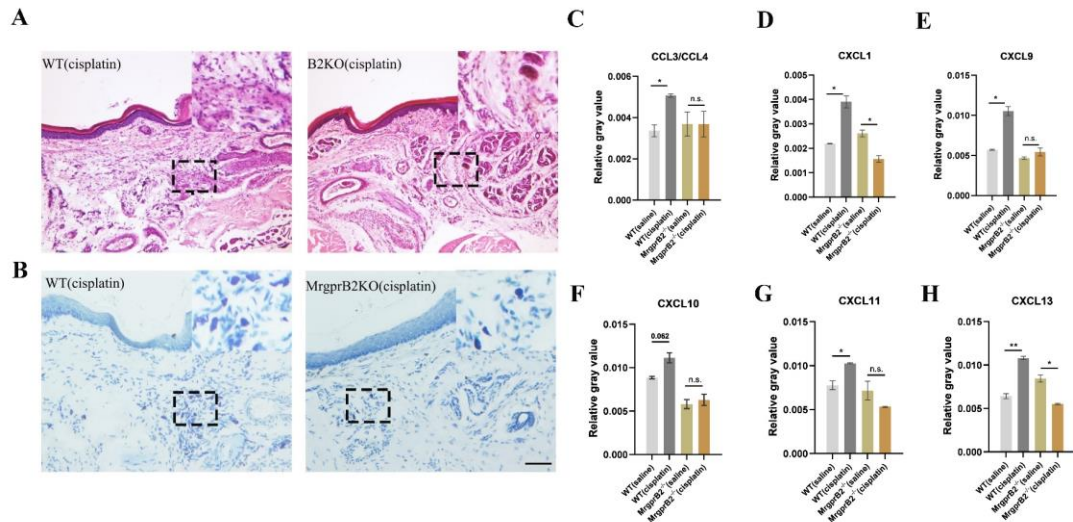
11 11, respectively (125 \times , scale bar was 100 μ m). (C-E) Cisplatin-induced pain was performed on WT

12 or Sash mice. Sash mice showed significant a decrease in cold allodynia induced by cisplatin (C),

13 but not in mechanical allodynia (D) and thermal hypersensitivity (E) Data were analyzed using two-
 14 tailed Student's t test, error bars show SEM, * $p < 0.05$, *** $p < 0.001$, $n = 5-6$.
 15



16
 17 **Figure S2** The ratio of weight loss in different model mice. (A) The ratio of weight loss in WT and
 18 Sash mice induced by cisplatin. (B) The ratio of weight loss in WT and MrgprB2^{-/-} female mice
 19 induced by cisplatin. (C) The ratio of weight loss in WT and MrgprB2^{-/-} male mice induced by
 20 cisplatin. (D) The ratio of weight loss in WT and MrgprD^{-/-} mice induced by cisplatin. Data were
 21 analyzed using two-tailed Student's t test, error bars show SEM, * $p < 0.05$, ** $p < 0.01$, $n = 5-6$.
 22



23

24 Figure S3 Knockout of MrgprB2 receptor reduces cisplatin-induced inflammatory cell infiltration.

25 (A) H&E staining showed that compared to C57BL/6J mice, MrgprB2^{-/-} mice had reductions in the

26 infiltration of inflammatory cells induced by cisplatin (200×, scale bar was 100 μm). (B) Toluidine

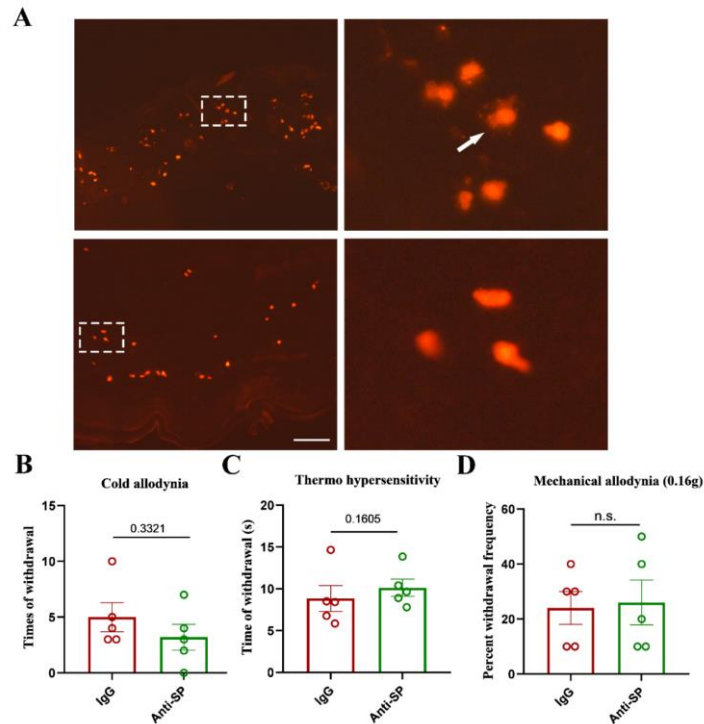
27 blue staining showed that compared to C57BL/6J mice, MrgprB2^{-/-} mice had reductions in the

28 infiltration of mast cells induced by cisplatin. (C-H) Inflammatory cytokines were assessed by the

29 Proteome Profiler Mouse XL Cytokine Array. The relative intensity of individual cytokines was

30 analyzed after normalizing to the positive controls on the same membrane.

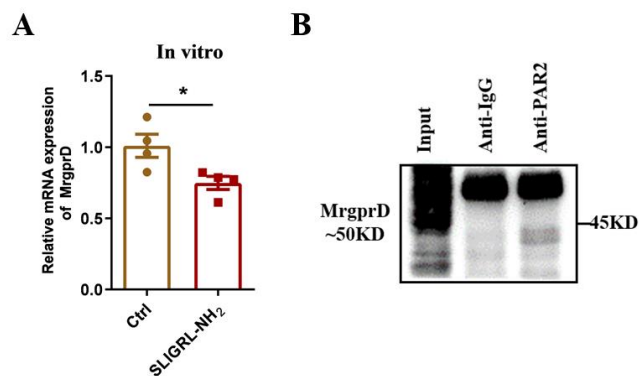
31



32

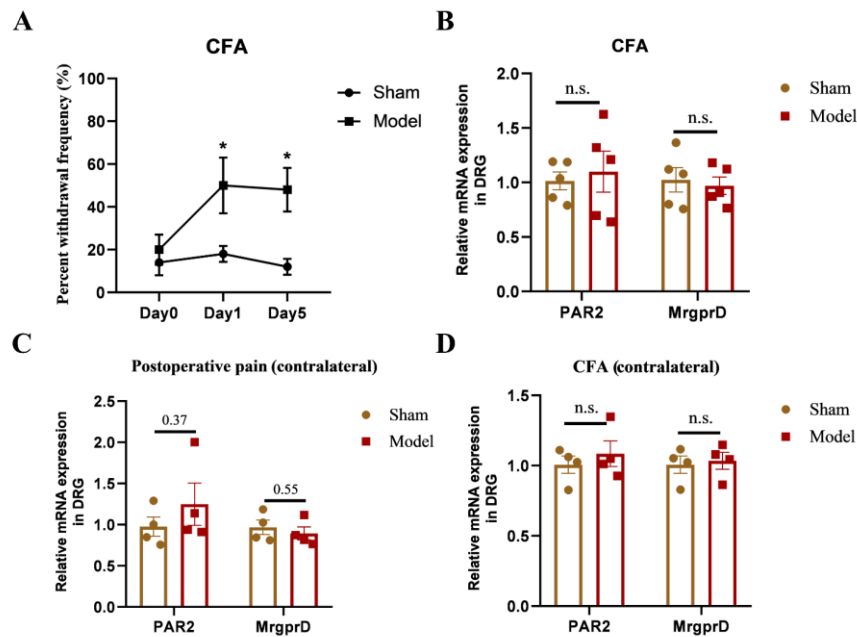
33 Figure S4 (A) Anti-substance P antibody treatment could alleviate MrgprB2⁺ mast cells
 34 degranulation. (B-D) Knockout of MrgprB2 receptor reduces the analgesic effect of anti-substance
 35 P antibody. Data were analyzed using two-tailed Student's t test, error bars show SEM, n = 5.

36



37

38 **Figure S5** (A) SLIGRL-NH₂ (100 μmol/L, 2 h) regulated MrgprD mRNA expression in whole DRG
 39 neurons isolated from WT mice. Data were analyzed using two-tailed Student's t test, error bars
 40 show SEM, * *p* < 0.05, n=4. (B) Total MrgprD (Lane 1) and Immunoprecipitated (IP) MrgprD (Lane
 41 2,3) were detected by Western Blotting.



43

44 **Figure S6 (A)** Behavioral tests of mechanical allodynia in CFA. Data were analyzed using two-45 tailed Student's t test, error bars show SEM, * $p < 0.05$, $n = 5$. (B) The mRNA expression of PAR2

46 and MrgprD in whole DRGs of CFA model at day 5. Data were analyzed using two-tailed Student's

47 t test, error bars show SEM, $n = 5$. (C) The mRNA expression of PAR2 and MrgprD in contralateral

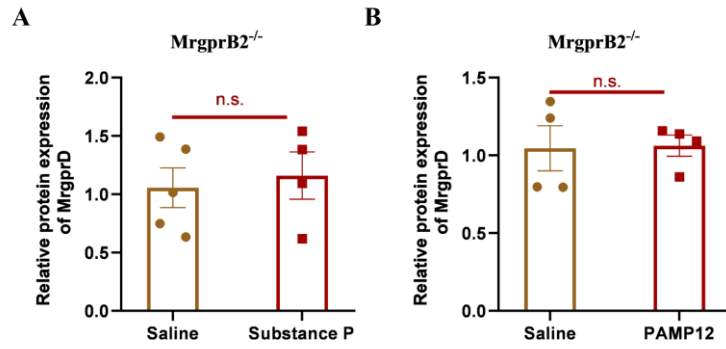
48 DRGs of postoperative pain model at day 5. Data were analyzed using two-tailed Student's t test,

49 error bars show SEM, $n = 4$. (D) The mRNA expression of PAR2 and MrgprD in contralateral DRGs

50 of CFA pain model at day 5. Data were analyzed using two-tailed Student's t test, error bars show

51 SEM, $n = 4$.

52



53

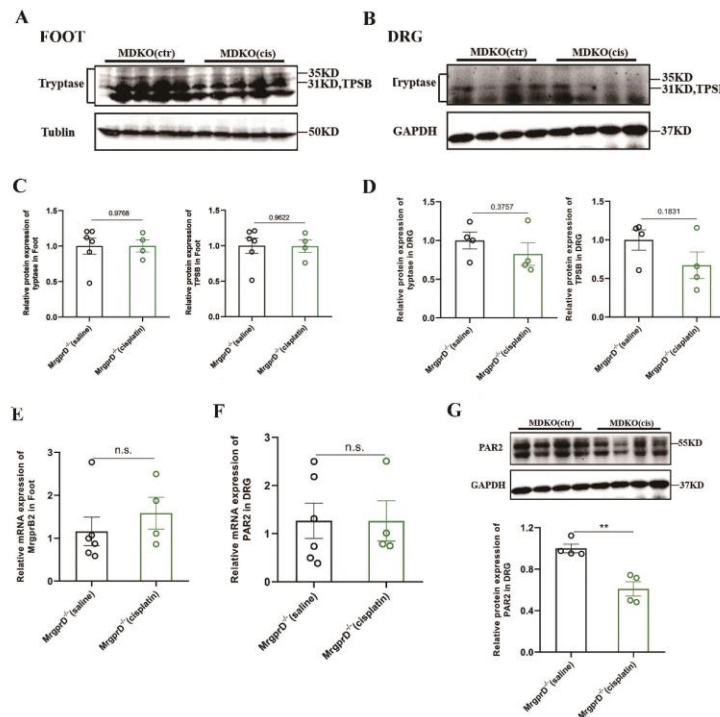
54 **Figure S7** (A) Effect of Substance P (10 µg/mouse, intradermal injection) stimulation for 2 hours

55 on MrgprD expression in DRGs of MrgprB2^{-/-} mice. (B) Effect of PAMP12 (40 µg/mouse,

56 intradermal injection) stimulation for 2 hours on MrgprD expression in DRGs of MrgprB2^{-/-}

57 mice. Data were analyzed using two-tailed Student's t test, error bars show SEM, n = 4-5.

58



59

60 **Figure S8** Knockout MrgprD reduces the upregulation of MrgprB2 induced by cisplatin. (A, C) The

61 expression of tryptase and β-tryptase was not increased in hindpaw tissues of MrgprD^{-/-} mice after

62 modeling. (B, D) The expression of tryptase and β-tryptase in whole DRGs was measured in

63 MrgprD^{-/-} mice (GAPDH band was shared with the internal reference in Figure S8G, and the
64 GAPDH band was washed by stripping buffer and then the anti-tryptase antibody was incubated).
65 (E) The MrgprB2 expression in hindpaw tissues was measured in MrgprD^{-/-} mice after modeling.
66 (F) The mRNA expression of PAR2 was measured in MrgprD^{-/-} mice after modeling. (G) The protein
67 expression of PAR2 in whole DRGs were measured in MrgprD^{-/-} mice. Data were analyzed using
68 two-tailed Student's t test, error bars show SEM, ** $p < 0.01$, n = 4-6.
69